



# Galactic Diffuse Gamma Rays and PeVatron Candidate Sources Observed by the Tibet AS $\gamma$ Experiment

Kazumasa KAWATA (ICRR, University of Tokyo)

For the Tibet AS $\gamma$  Collaboration





# Tibet AS $\gamma$ Collaboration



M. Amenomori<sup>1</sup>, S. Asano<sup>2</sup>, Y. W. Bao<sup>3</sup>, X. J. Bi<sup>4</sup>, D. Chen<sup>5</sup>, T. L. Chen<sup>6</sup>, W. Y. Chen<sup>4</sup>, Xu Chen<sup>4,5</sup>, Y. Chen<sup>3</sup>, Cirennima<sup>6</sup>, S. W. Cui<sup>7</sup>, Danzengluobu<sup>6</sup>, L. K. Ding<sup>4</sup>, J. H. Fang<sup>4,8</sup>, K. Fang<sup>4</sup>, C. F. Feng<sup>9</sup>, Zhaoyang Feng<sup>4</sup>, Z. Y. Feng<sup>10</sup>, Qi Gao<sup>6</sup>, A. Gomi<sup>11</sup>, Q. B. Gou<sup>4</sup>, Y. Q. Guo<sup>4</sup>, Y. Y. Guo<sup>4</sup>, Y. Hayashi<sup>2</sup>, H. H. He<sup>4</sup>, Z. T. He<sup>7</sup>, K. Hibino<sup>12</sup>, N. Hotta<sup>13</sup>, Haibing Hu<sup>6</sup>, H. B. Hu<sup>4</sup>, K. Y. Hu<sup>4,8</sup>, J. Huang<sup>4</sup>, H. Y. Jia<sup>10</sup>, L. Jiang<sup>4</sup>, P. Jiang<sup>5</sup>, H. B. Jin<sup>5</sup>, K. Kasahara<sup>14</sup>, Y. Katayose<sup>11</sup>, C. Kato<sup>2</sup>, S. Kato<sup>15</sup>, I. Kawahara<sup>11</sup>, T. Kawashima<sup>15</sup>, K. Kawata<sup>15</sup>, M. Kozai<sup>16</sup>, D. Kurashige<sup>11</sup>, Labaciren<sup>6</sup>, G. M. Le<sup>17</sup>, A. F. Li<sup>4,9,18</sup>, H. J. Li<sup>6</sup>, W. J. Li<sup>4,10</sup>, Y. Li<sup>5</sup>, Y. H. Lin<sup>4,8</sup>, B. Liu<sup>19</sup>, C. Liu<sup>4</sup>, J. S. Liu<sup>4</sup>, L. Y. Liu<sup>5</sup>, M. Y. Liu<sup>6</sup>, W. Liu<sup>4</sup>, X. L. Liu<sup>5</sup>, Y.-Q. Lou<sup>20,21,22</sup>, H. Lu<sup>4</sup>, X. R. Meng<sup>6</sup>, Y. Meng<sup>4,8</sup>, K. Munakata<sup>2</sup>, K. Nagaya<sup>11</sup>, Y. Nakamura<sup>15</sup>, Y. Nakazawa<sup>23</sup>, H. Nanjo<sup>1</sup>, C. C. Ning<sup>6</sup>, M. Nishizawa<sup>24</sup>, R. Noguchi<sup>11</sup>, M. Ohnishi<sup>15</sup>, S. Okukawa<sup>11</sup>, S. Ozawa<sup>25</sup>, L. Qian<sup>5</sup>, X. Qian<sup>5</sup>, X. L. Qian<sup>26</sup>, X. B. Qu<sup>27</sup>, T. Saito<sup>28</sup>, Y. Sakakibara<sup>11</sup>, M. Sakata<sup>29</sup>, T. Sako<sup>15</sup>, T. K. Sako<sup>15</sup>, T. Sasaki<sup>12</sup>, J. Shao<sup>4,9</sup>, M. Shibata<sup>11</sup>, A. Shiomi<sup>23</sup>, H. Sugimoto<sup>30</sup>, W. Takano<sup>12</sup>, M. Takita<sup>15</sup>, Y. H. Tan<sup>4</sup>, N. Tateyama<sup>12</sup>, S. Torii<sup>31</sup>, H. Tsuchiya<sup>32</sup>, S. Udo<sup>12</sup>, H. Wang<sup>4</sup>, Y. P. Wang<sup>6</sup>, Wangdai<sup>6</sup>, H. R. Wu<sup>4</sup>, Q. Wu<sup>6</sup>, J. L. Xu<sup>5</sup>, L. Xue<sup>9</sup>, Z. Yang<sup>4</sup>, Y. Q. Yao<sup>5</sup>, J. Yin<sup>5</sup>, Y. Yokoe<sup>15</sup>, N. P. Yu<sup>5</sup>, A. F. Yuan<sup>6</sup>, L. M. Zhai<sup>5</sup>, C. P. Zhang<sup>5</sup>, H. M. Zhang<sup>4</sup>, J. L. Zhang<sup>4</sup>, X. Zhang<sup>3</sup>, X. Y. Zhang<sup>9</sup>, Y. Zhang<sup>4</sup>, Yi Zhang<sup>33</sup>, Ying Zhang<sup>4</sup>, S. P. Zhao<sup>4</sup>, Zhaxisangzhu<sup>6</sup>, X. X. Zhou<sup>10</sup> and Y. H. Zou<sup>4,8</sup>

1 Department of Physics, Hirosaki Univ., Japan.

2 Department of Physics, Shinshu Univ., Japan.

3 School of Astronomy and Space Science, Nanjing Univ., China.

4 Key Laboratory of Particle Astrophysics, Institute of High Energy Physics, CAS, China.

5 National Astronomical Observatories, CAS, China.

6 Department of Mathematics and Physics, Tibet Univ., China.

7 Department of Physics, Hebei Normal Univ., China.

8 Univ. of Chinese Academy of Sciences, China.

9 Institute of Frontier and Interdisciplinary Science and Key Laboratory of Particle Physics and Particle Irradiation (MOE), Shandong Univ., China.

10 Institute of Modern Physics, SouthWest Jiaotong Univ., China.

11 Faculty of Engineering, Yokohama National Univ., Japan.

12 Faculty of Engineering, Kanagawa Univ., Japan.

13 Faculty of Education, Utsunomiya Univ., Japan.

14 Faculty of Systems Engineering, Shibaura Institute of Technology, Japan.

15 Institute for Cosmic Ray Research, Univ. of Tokyo, Japan.

16 Polar Environment Data Science Center, Joint Support-Center for Data Science Research, Research Organization of Information and Systems, Japan.

17 National Center for Space Weather, China Meteorological Administration, China.

18 School of Information Science and Engineering, Shandong Agriculture Univ., China.

19 Department of Astronomy, School of Physical Sciences, Univ. of Science and Technology of China, China.

20 Department of Physics and Tsinghua Centre for Astrophysics (THCA), Tsinghua Univ., China.

21 Tsinghua Univ.-National Astronomical Observatories of China (NAOC) Joint Research Center for Astrophysics, Tsinghua Univ., China.

22 Department of Astronomy, Tsinghua Univ., China.

23 College of Industrial Technology, Nihon Univ., Japan.

24 National Institute of Informatics, Japan.

25 National Institute of Information and Communications Technology, Japan.

26 Department of Mechanical and Electrical Engineering, Shandong Management Univ., China.

27 College of Science, China Univ. of Petroleum, China.

28 Tokyo Metropolitan College of Industrial Technology, Japan.

29 Department of Physics, Konan Univ., Japan.

30 Shonan Institute of Technology, Japan.

31 Research Institute for Science and Engineering, Waseda Univ., Japan.

32 Japan Atomic Energy Agency, TJapan.

33 Key Laboratory of Dark Matter and Space Astronomy, Purple Mountain Observatory, CAS, China.



# Tibet Air Shower Array

$\gamma/\text{CR}$

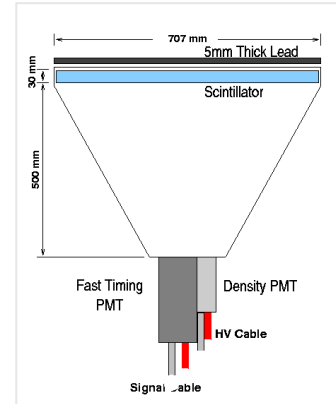
Air Shower



■ Site: Tibet ( $90.522^{\circ}\text{E}$ ,  $30.102^{\circ}\text{N}$ ) 4,300 m a.s.l.

## Present Performance

- ✓ # of detectors       $0.5 \text{ m}^2 \times 597$
- ✓ Covering area       $\sim 65,700 \text{ m}^2$
- ✓ Angular resolution       $\sim 0.5^{\circ} @ 10\text{TeV} \gamma$   
                                 $\sim 0.2^{\circ} @ 100\text{TeV} \gamma$
- ✓ Energy resolution       $\sim 40\% @ 10\text{TeV} \gamma$   
                                 $\sim 20\% @ 100\text{TeV} \gamma$

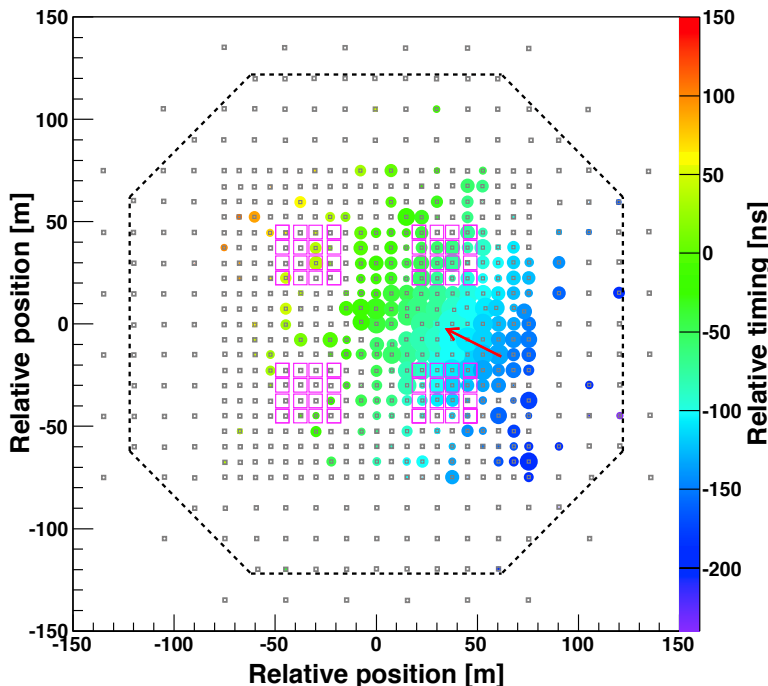


→ Observation of secondary (mainly  $e^{+/-}, \gamma$ ) in AS  
Primary energy : 2<sup>nd</sup> particle densities  
Primary direction : 2<sup>nd</sup> relative timings



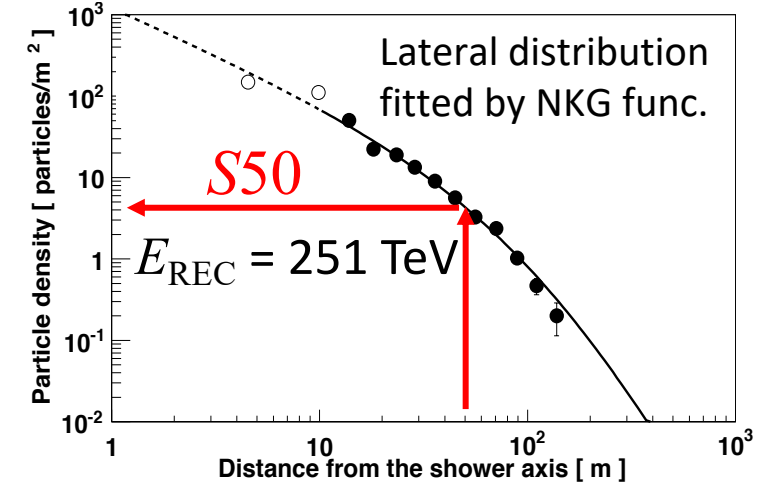
# Air Shower Reconstruction

Gamma-ray candidate event



circle size  $\propto \log(\# \text{ of detected particles})$   
circle color  $\propto \text{relative timing [ns]}$

*Amenomori +, PRL 123, 051101 (2019)*



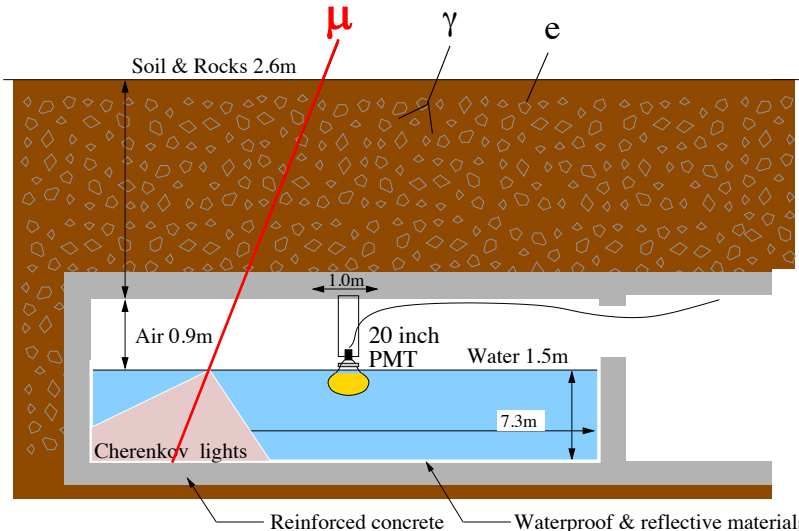
S50 improves  $E$  resolutions (10 - 1000 TeV)  
 $\rightarrow \sim 40\% @ 10 \text{ TeV}, \sim 20\% @ 100 \text{ TeV}$

*Kawata +, Experimental Astronomy 44, 1 (2017)*



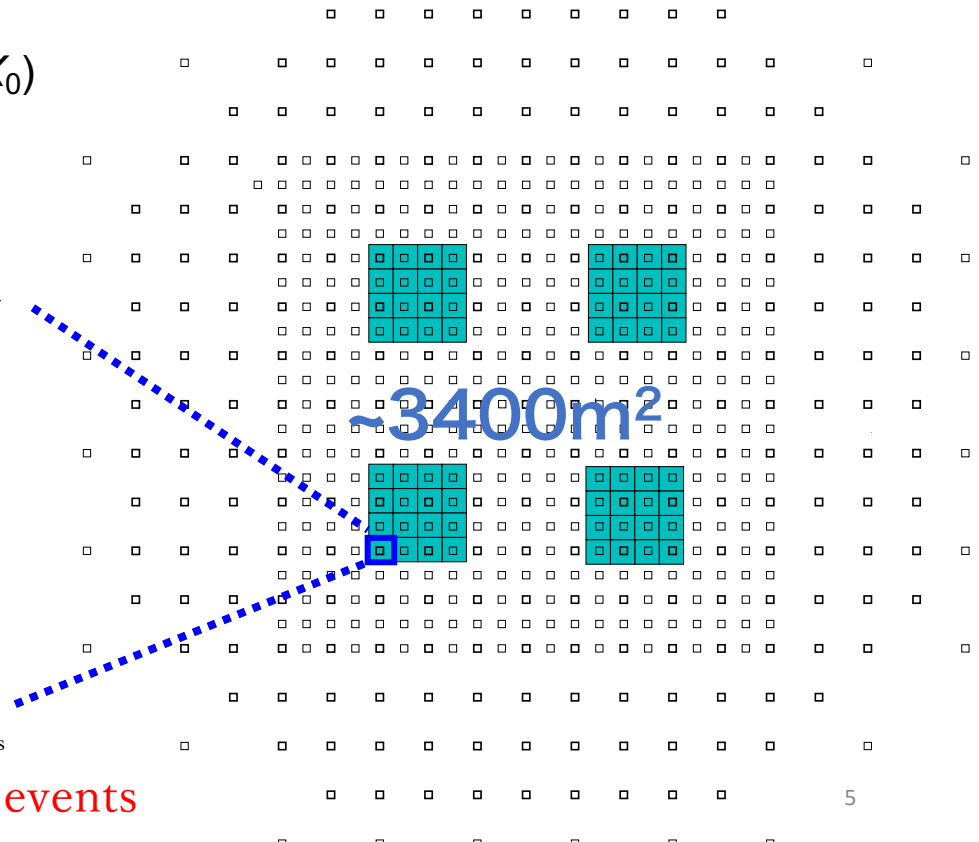
# Underground WC Muon Detectors

- ✓ 4 pools, 16 units / pool
- ✓  $54 \text{ m}^2$  in area  $\times 1.5\text{m}$  in depth / unit
- ✓ 2.4m soil overburden ( $\sim 515\text{g/cm}^2 \sim 9X_0$ )
- ✓ 20"ΦPMT (HAMAMATSU R3600)
- ✓ Concrete pools + white Tyvek sheets



→ Succeeded in rejecting by  $>99.9\%$  CR events

Measurement of # of  $\mu$  in AS  $\rightarrow \gamma/\text{CR}$  discrimination  
DATA: February 2014 - May 2017 **Live time: 719 days**

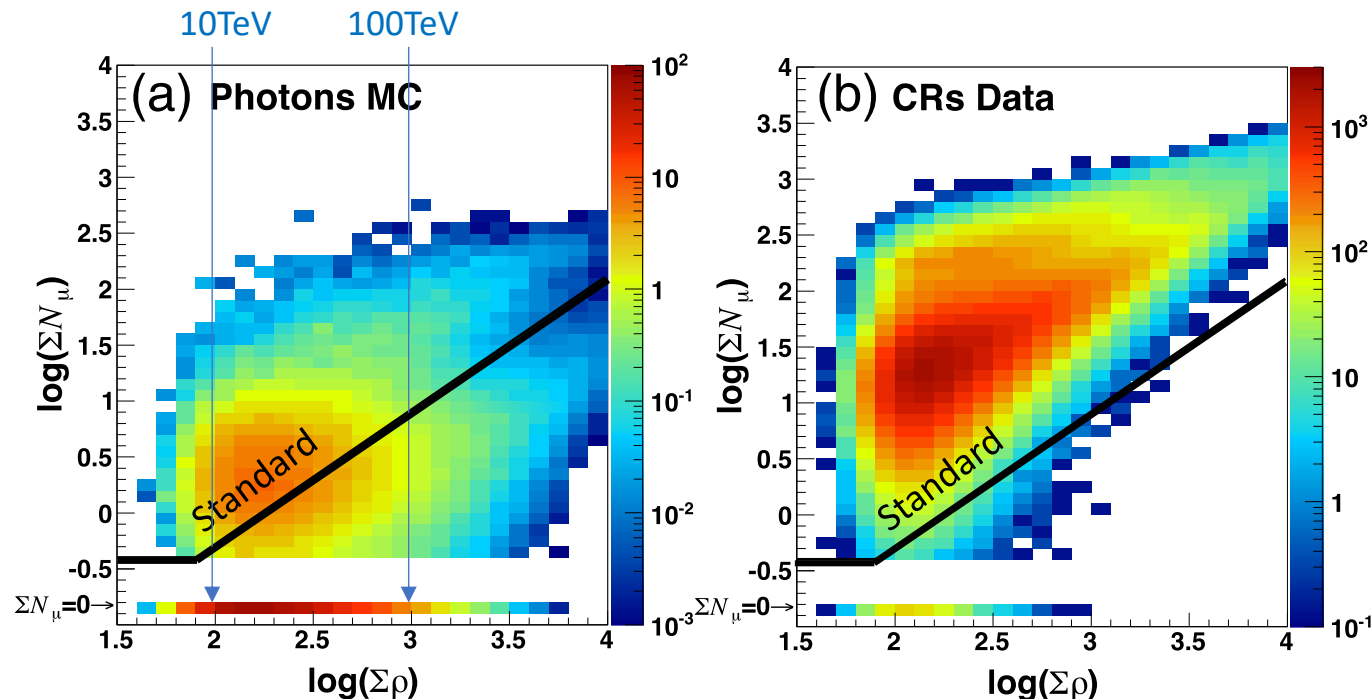




# Muon Cut Condition (Standard)

Standard muon cut :  $\Sigma N_\mu < 2.1 \times 10^{-3} \Sigma \rho^{1.2}$

→ Optimized for the gamma-ray point-like source



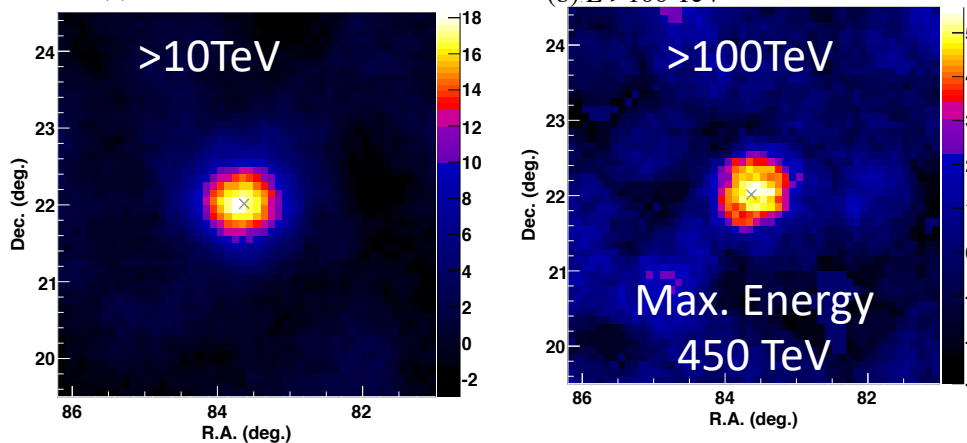
Gamma Survival ratio : ~90% by MC sim (>100TeV)

CR Survival ratio : ~ $10^{-3}$  (>100TeV)



# UHE $\gamma$ -rays from the Crab Nebula (2019)

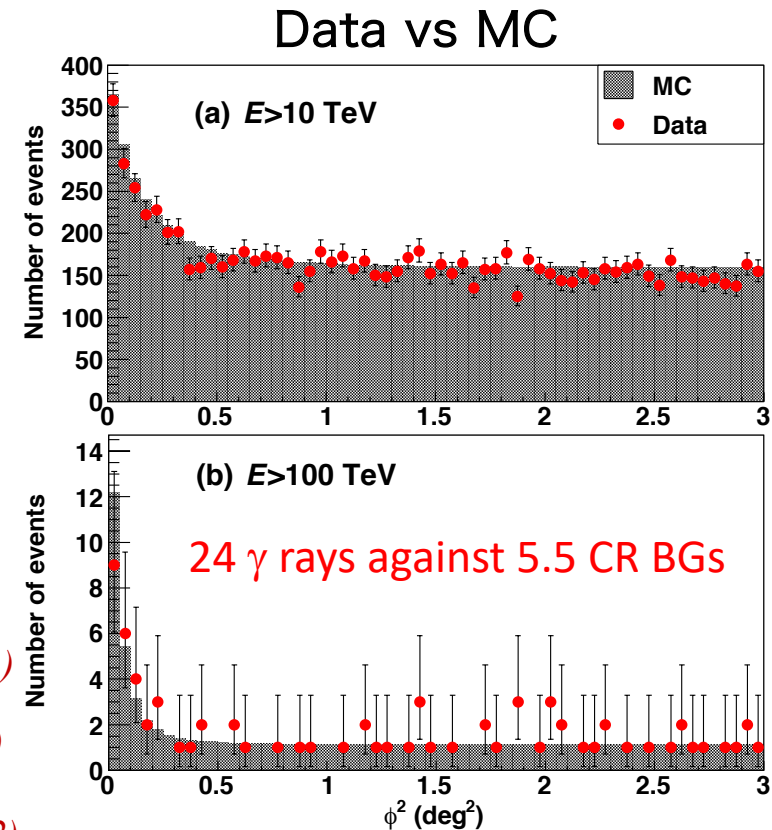
*Amenomori et al., PRL 123, 051101 (2019)*



First Detection of Sub-PeV  $\gamma$  ( $5.6\sigma$ )

Other detected sources in 100 TeV region

- ✓ G106.3+2.7 *Amenomori et al., Nat. Astron, 5, 460 (2021)*
- ✓ Cygnus OB1 *Amenomori et al., PRL, 127, 031102 (2021)*
- ✓ Cygnus OB2
- ✓ HESS J1843-033 *Amenomori et al., ApJ, 932, 120 (2022)*
- ✓ HESS J1849-000 *Accepted (2023)*

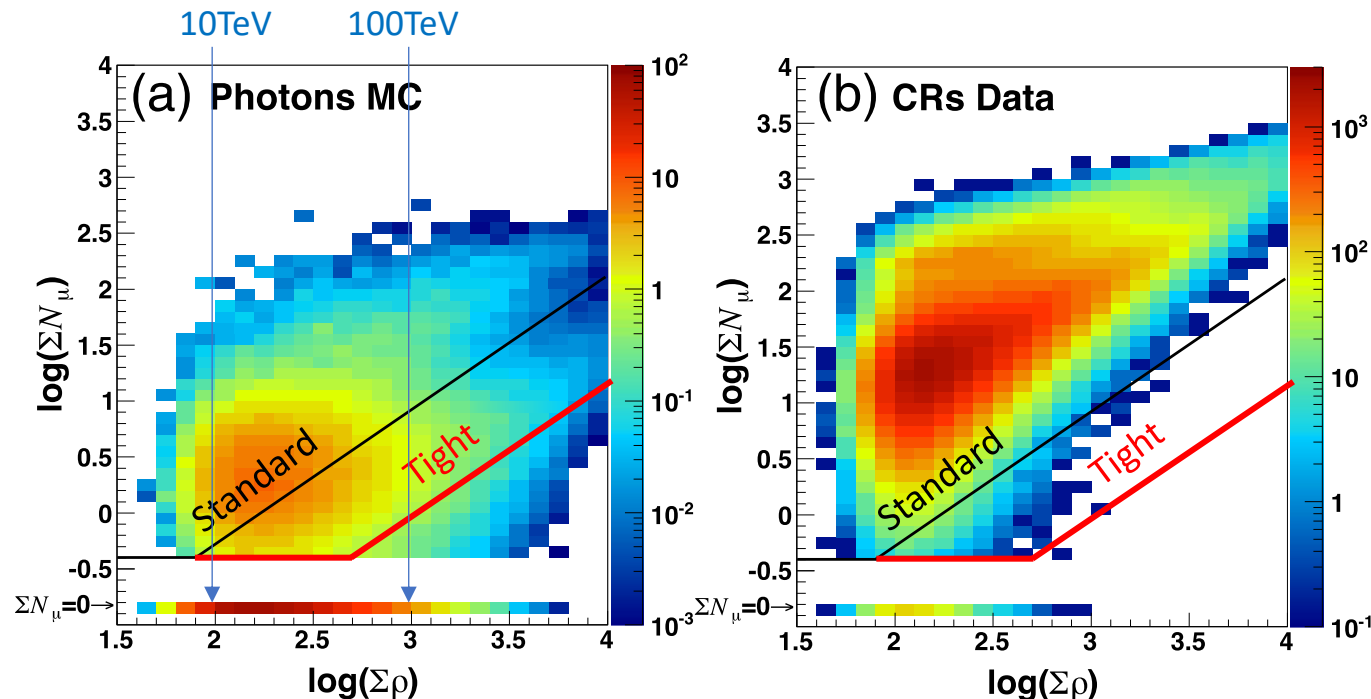




# Muon Cut Condition (Tight) for Diffuse $\gamma$

Tight muon cut :  $\Sigma N_\mu < 2.1 \times 10^{-4} \Sigma \rho^{1.2}$

→ One order magnitude tighter than the Crab analysis



Gamma Survival ratio : ~30% by MC sim (>398TeV)

CR Survival ratio : ~ $10^{-6}$  (>398TeV =  $10^{2.6}$ TeV)



# $\gamma$ -ray-like event Distribution

Gamma-ray-like events  
after the tight muon cut  
in the equatorial coordinates

Blue points:

Experimental data

Red plus marks:

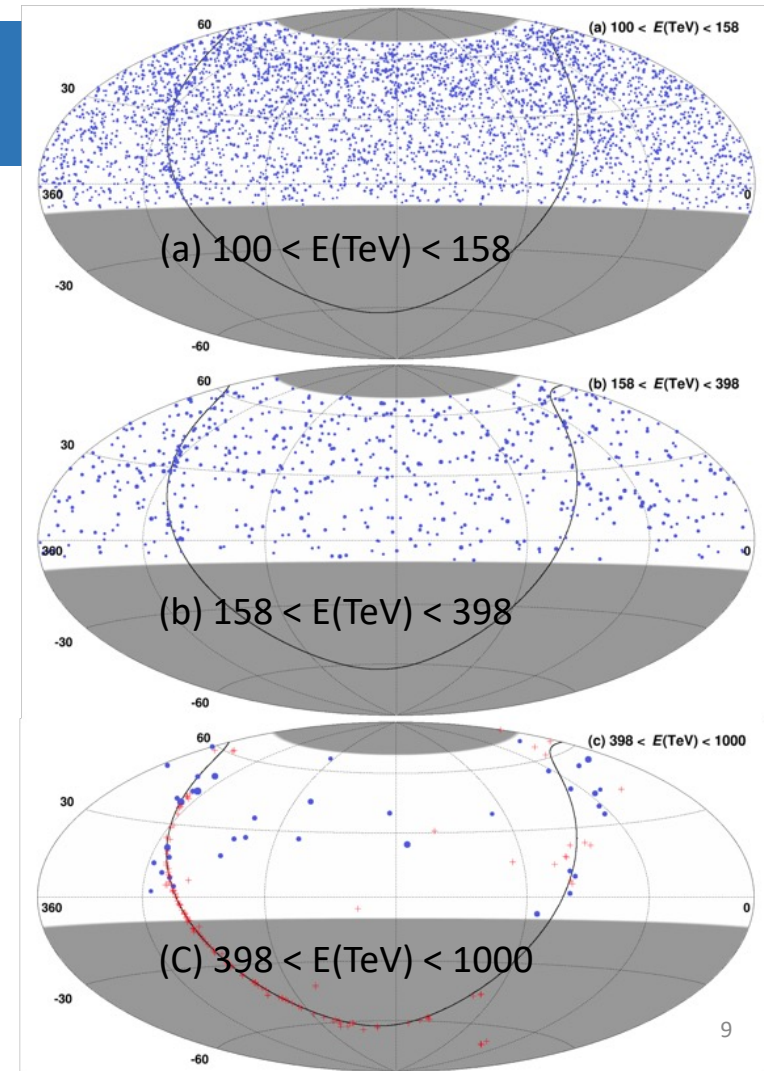
known Galactic TeV sources

>398 TeV ( $10^{2.6}$  TeV)

38 events in our FoV

23 events in  $|b| < 10^\circ$

16 events in  $|b| < 5^\circ$





# Latitude Profile

6.6 $\sigma$

Amenomori et al., PRL 126, 141101 (2021)

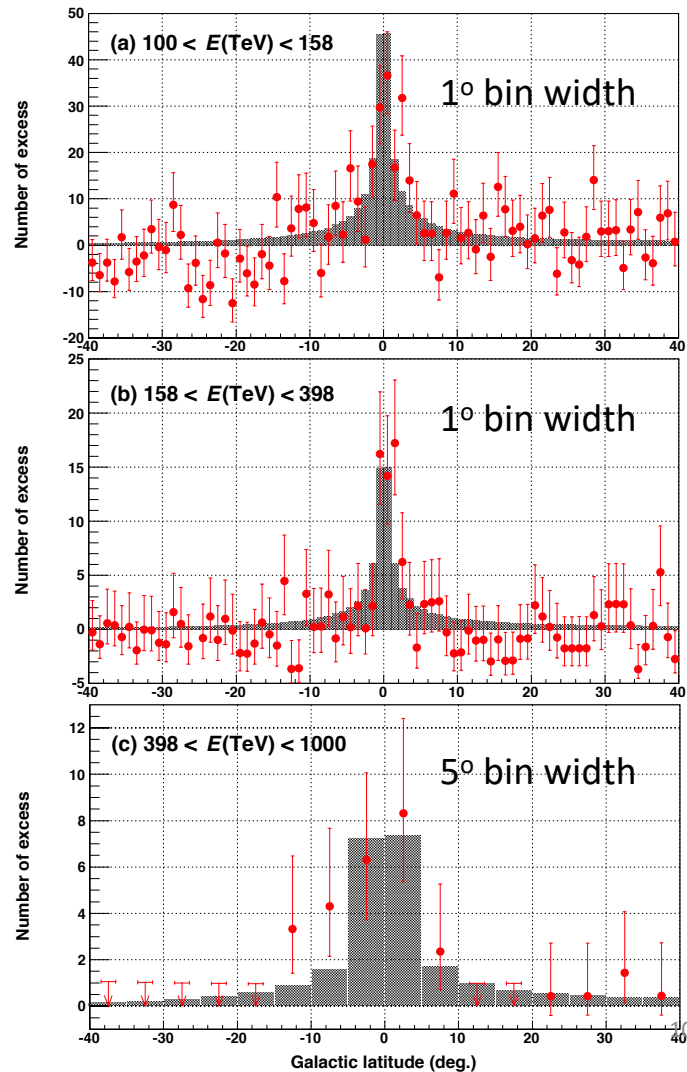
Red points:  
experimental data across  
our FoV ( $22^\circ < l < 225^\circ$ )  
including source contribution

Gray shade histogram:  
Model by Lipari and Vernetto

Lipari & Vernetto, PRD 98, 043003 (2018)

5.9 $\sigma$

5.1 $\sigma$





# Energy Spectrum of UHE Diffuse $\gamma$ Rays

Amenomori et al., PRL 126, 141101 (2021)

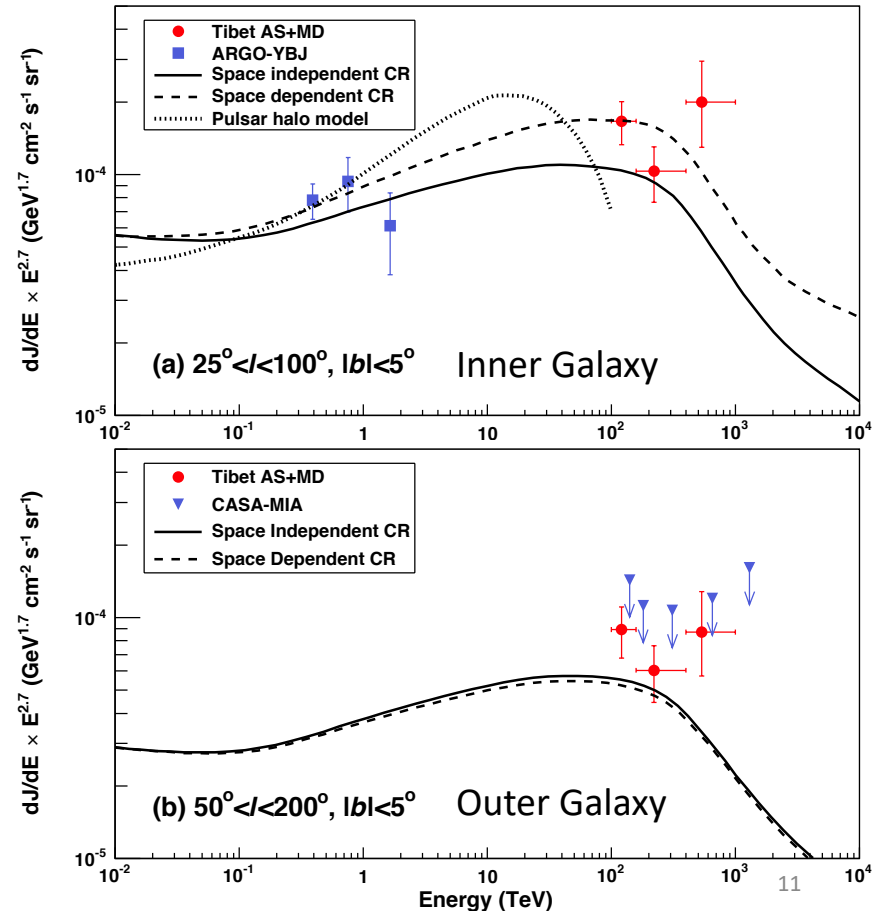
After excluding the contribution from the known TeV sources (within 0.5 degrees) listed in the TeV source catalog



The measured fluxes are overall consistent with Lipari's diffuse gamma model assuming the hadronic cosmic ray origin.



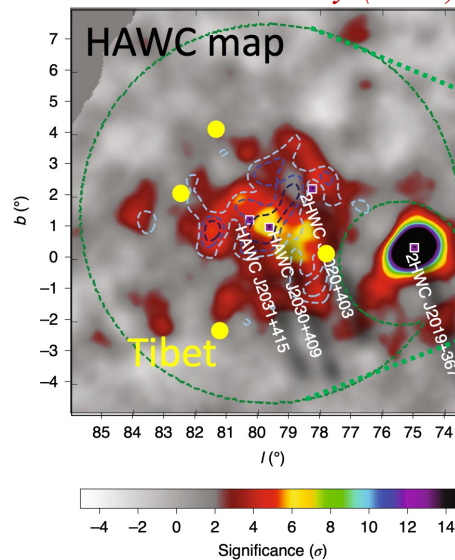
Lipari & Vernetto, PRD 98, 043003 (2018)



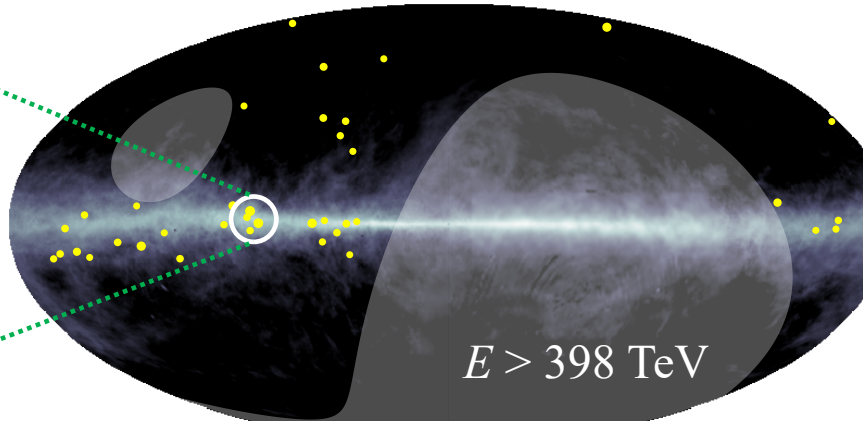


# PeVatron Candidate: Cygnus Cocoon

*Abeysekara et al.,  
Nature Astronomy (2021)*

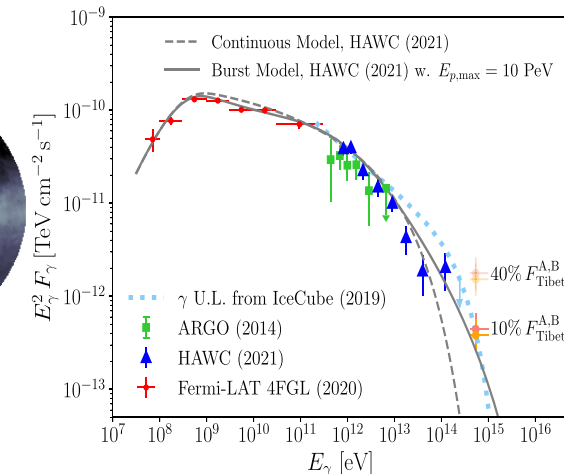


*Amenomori et al., PRL 126, 141101 (2021)*



Galactic Coordinates

*Fang & Murase,  
ApJ, 919, 93 (2021)*

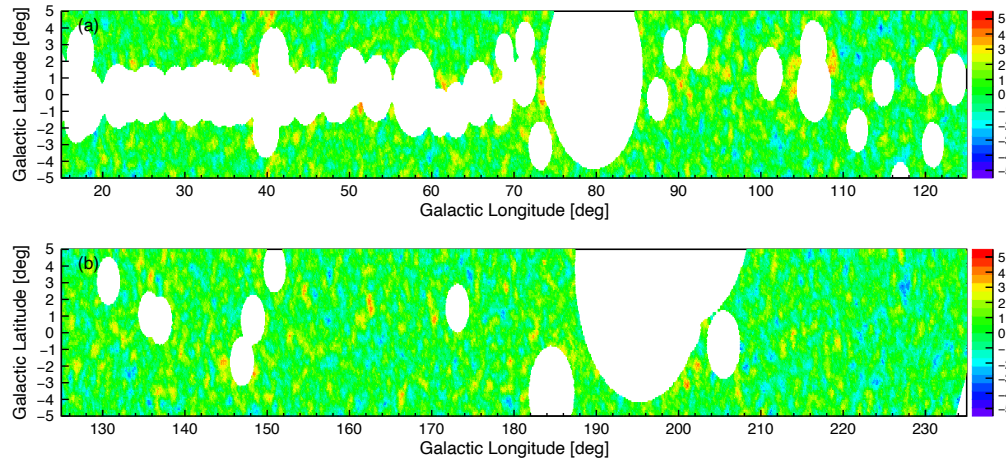


4 events above 398 TeV detected within 4°-radius-circle from the **Cygnus cocoon** which is claimed as an extended source by the ARGO-YBJ and HAWC and also proposed as a candidate of the PeVatrons.



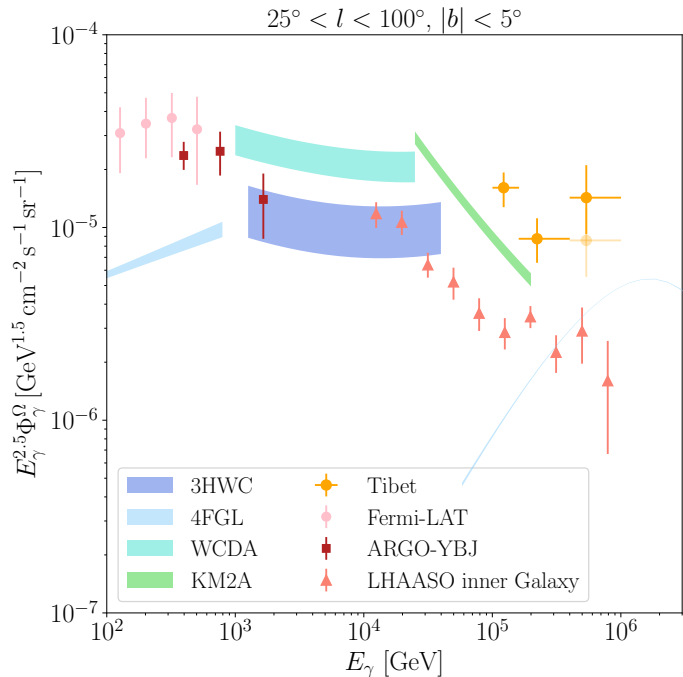
# LHAASO Diffuse Gamma Rays

Z. Cao et al. :arXiv:2305.05372v1



LHAASO flux: a few times lower than Tibet flux,  
but not directly compared, due to the large  
masked regions by LHAASO.

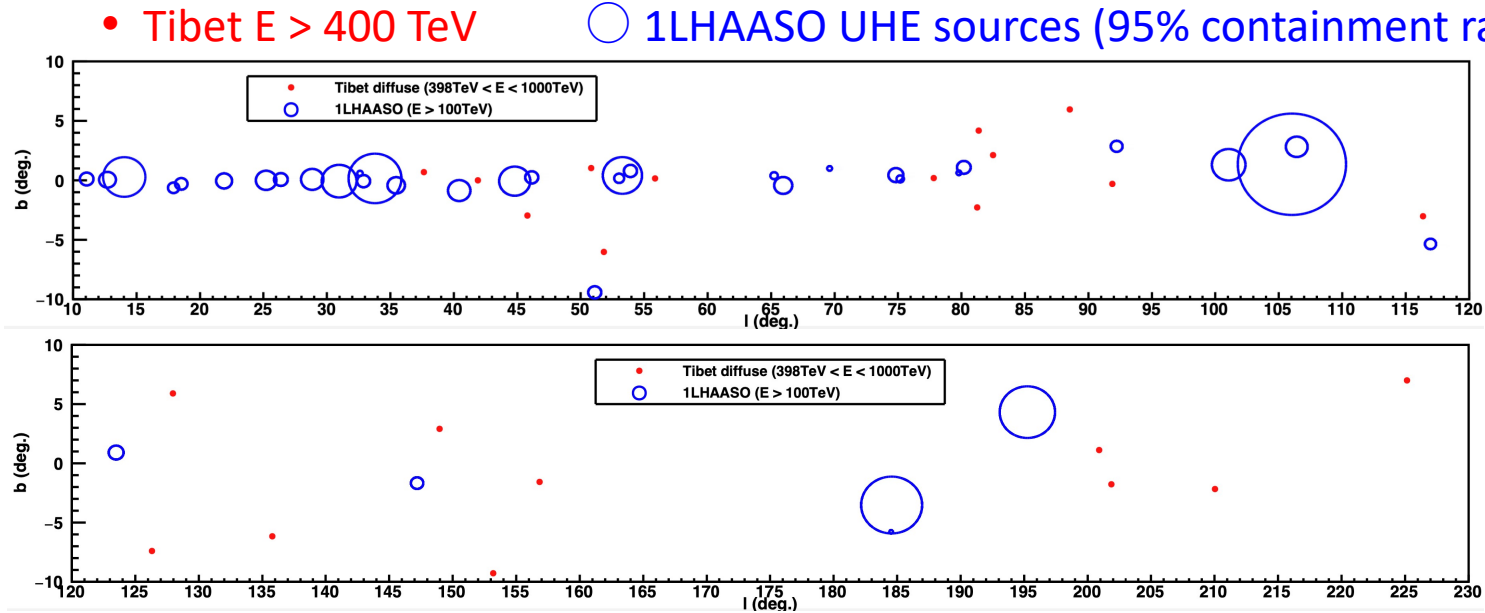
K. Fang & K. Murase :arXiv:2307.02905v1





# 1LHAASO Catalog and Tibet UHE Events

Z. Cao et al. :arXiv:2305.17030v1



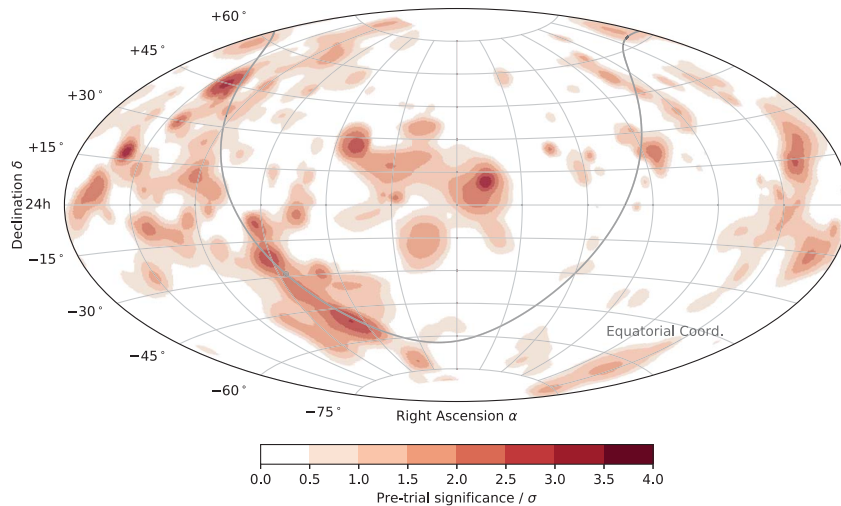
Tibet Galactic diffuse gamma rays above 400 TeV:  
do NOT originate from 1LHAASO UHE ( $>100$  TeV) sources.



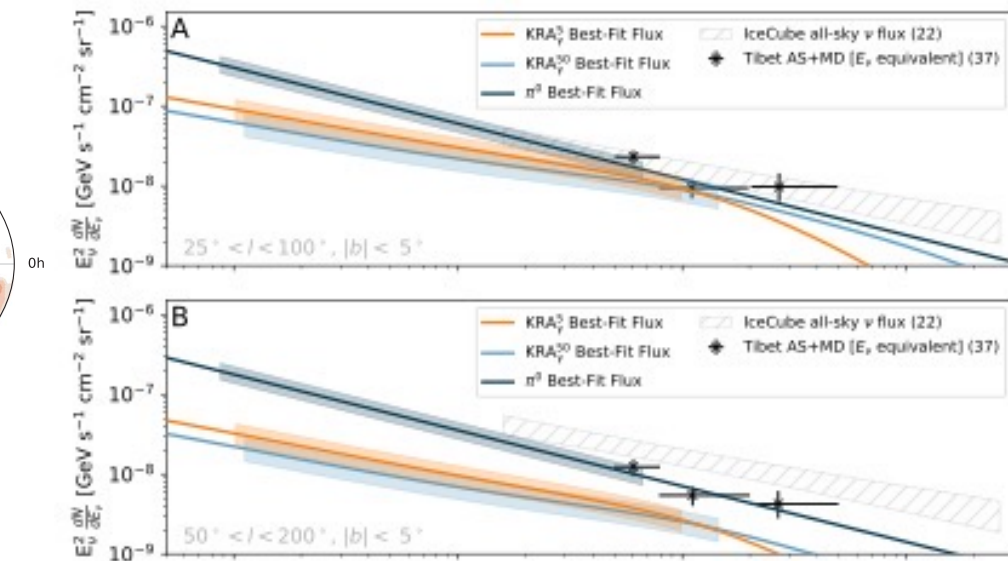
# IceCube Diffuse Neutrinos

*IceCube Collaboration: Science, 380, 1338 (2023)*

4.5 $\sigma$  at Galactic plane



Comparison with Tibet diffuse  $\gamma$ -rays

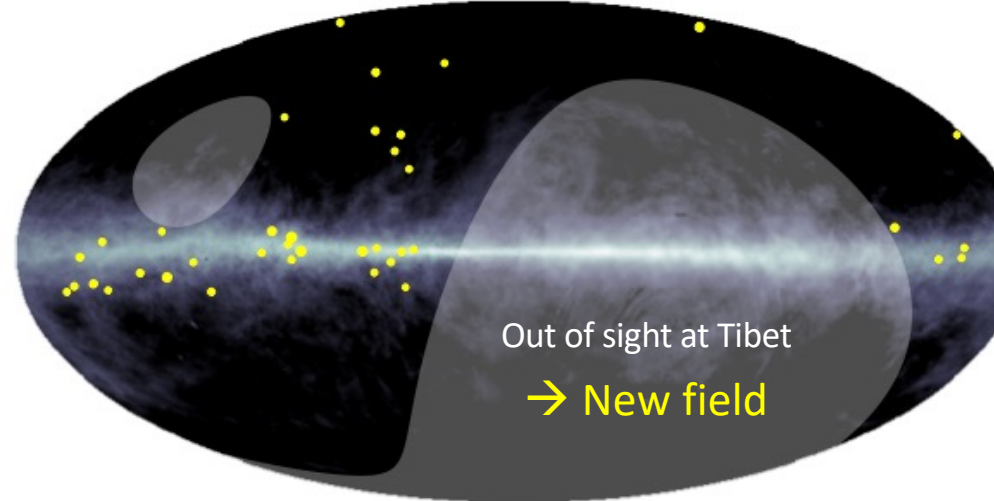


IceCube  $\nu$  flux smoothly connects to the  $\nu$  flux estimated from the Tibet sub-PeV  $\gamma$ -ray flux, assuming  $\pi^0$ -model best-fit flux supporting cosmic-ray origin of Tibet sub-PeV galactic diffuse  $\gamma$  rays.



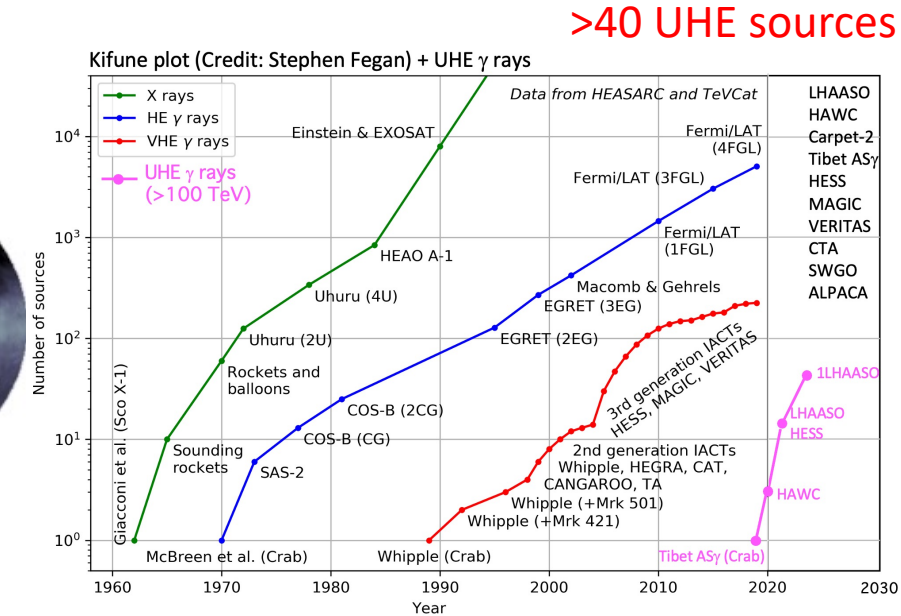
# Projects in the Southern Hemisphere

UHE diffuse gamma rays



Go South!

(e.g., ALPACA [2022-24], Mega ALPACA, SWGO, CTA, ...) & Neutrinos



Draw the "Kifune" plot - the integral number of high energy sources detected as a function of year - in the style of a plot developed by Tadashi Kifune (for example [http://adsabs.harvard.edu/abs/1996NCimC\\_19\\_953](http://adsabs.harvard.edu/abs/1996NCimC_19_953)).

The data for the number of X-ray and HE (GeV) gamma-ray sources come from a page on HEASARC maintained by Stephen A. Drake (retrieved 2017-09-28) : [https://heasarc.gsfc.nasa.gov/docs/heasarc/headates/how\\_many\\_xray.html](https://heasarc.gsfc.nasa.gov/docs/heasarc/headates/how_many_xray.html)

The data for the number of VHE (TeV) gamma-ray sources is from TeVCat maintained by Deirdre Horan and Scott Wakely (retrieved 2017-05-28) : <http://tevcat.uchicago.edu/>



# Conclusions

- ✓ Tibet AS $\gamma$  experiment successfully observed UHE gamma rays from the Crab Nebula for the first time and opened new energy window. (Now >40 UHE  $\gamma$  ray sources detected by LHAASO, HAWC, H.E.S.S. and Tibet AS $\gamma$  )
- ✓ Tibet AS $\gamma$  experiment successfully observed Galactic diffuse gamma rays between 100 TeV and 1 PeV for the first time.
- ✓ Tibet UHE events (>400 TeV) do not originate from LHAASO UHE (>100 TeV) sources.
- ✓ IceCube diffuse neutrino flux smoothly connects to Tibet AS $\gamma$  diffuse gamma-ray flux assuming  $\pi^0$  best-fit model supporting the cosmic-ray origin.

These facts indicate strong evidence that cosmic rays are accelerated beyond PeV energies in our Galaxy and spread over the Galactic disk.  
→ Search for current active PeVatrons! → Go South!

# Backup slides



# Composition Dependence

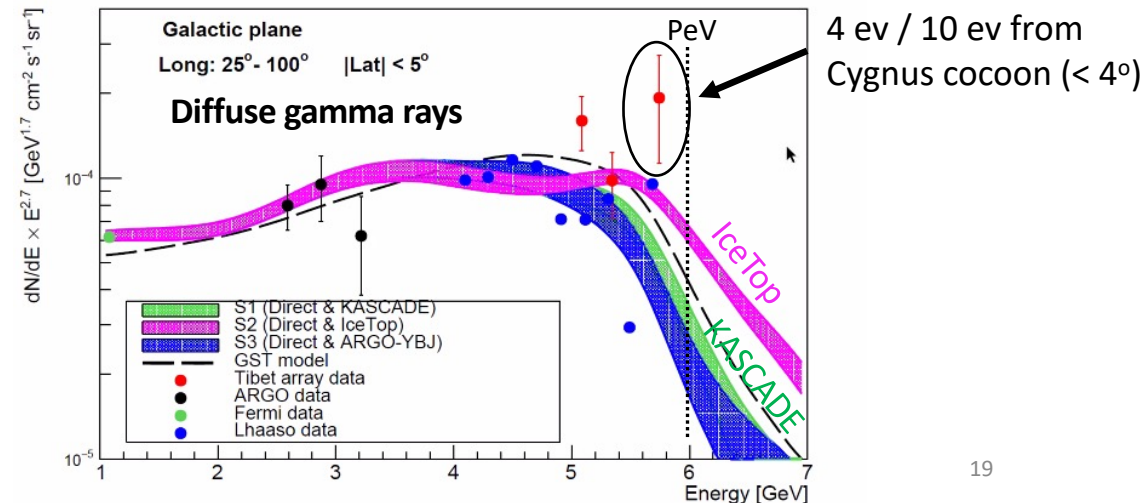
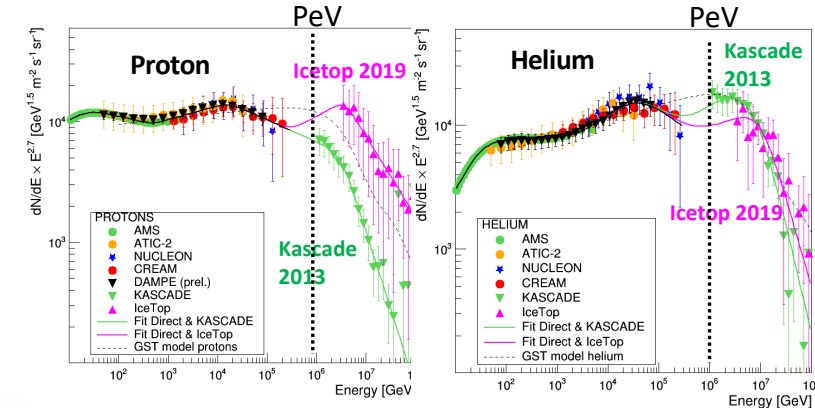
CRs interact with interstellar gas  
( $\gamma$ -ray energy has 10% of CRs)



→ Diffuse gamma-ray spectrum depends on the CR composition

*Vernetto & Lipari (ICRC2021)*

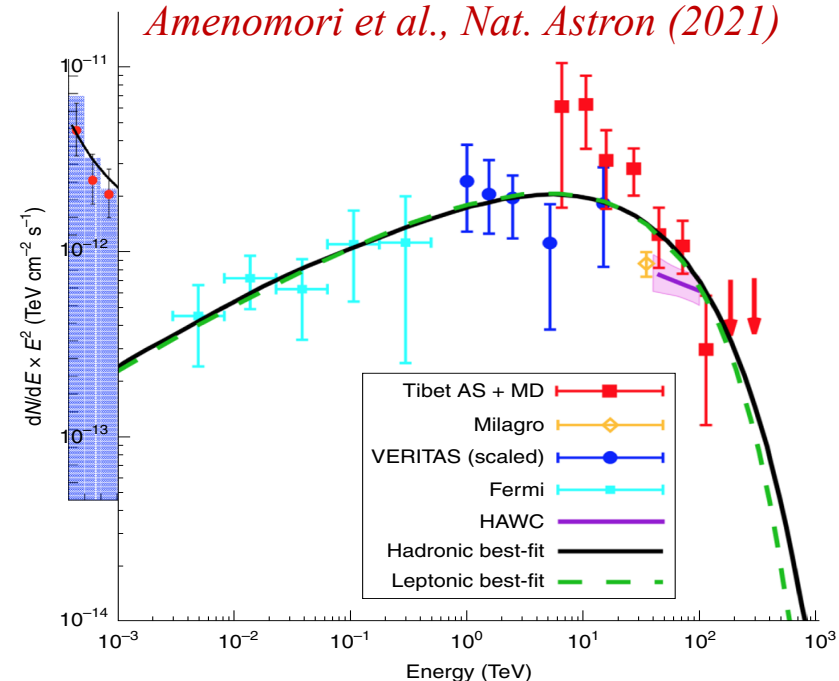
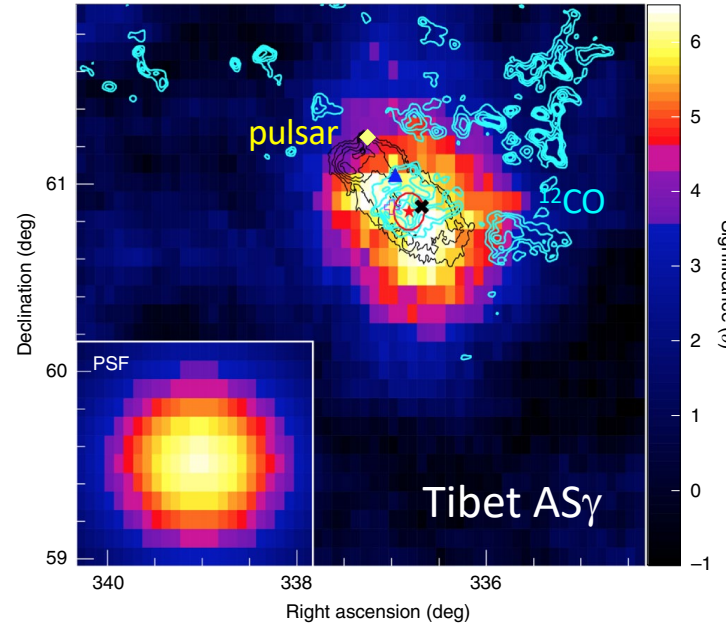
factor 1.5 – 2 difference@~600 TeV





# PeVatron Candidate: SNR G106.3+2.7

Detected by  
VERITAS,  
HAWC,  
Tibet AS $\gamma$ ,  
MAGIC,  
LHAASO



- ✓ Spectrum extends beyond 100 TeV (HAWC, Tibet AS $\gamma$ , LHAASO)
- ✓ Shell-type SNR near the pulsar ( $t_{\text{age}} \sim 10 \text{ kyr}$ ?,  $d = 800 \text{ pc}$ ?)
- ✓ Extended  $\gamma$ -ray excess ( $\sigma_{\text{EXT}} = 0.24^\circ \pm 0.10^\circ$ )
- ✓  $\gamma$ -ray excess is coincident with the could, not pulsar

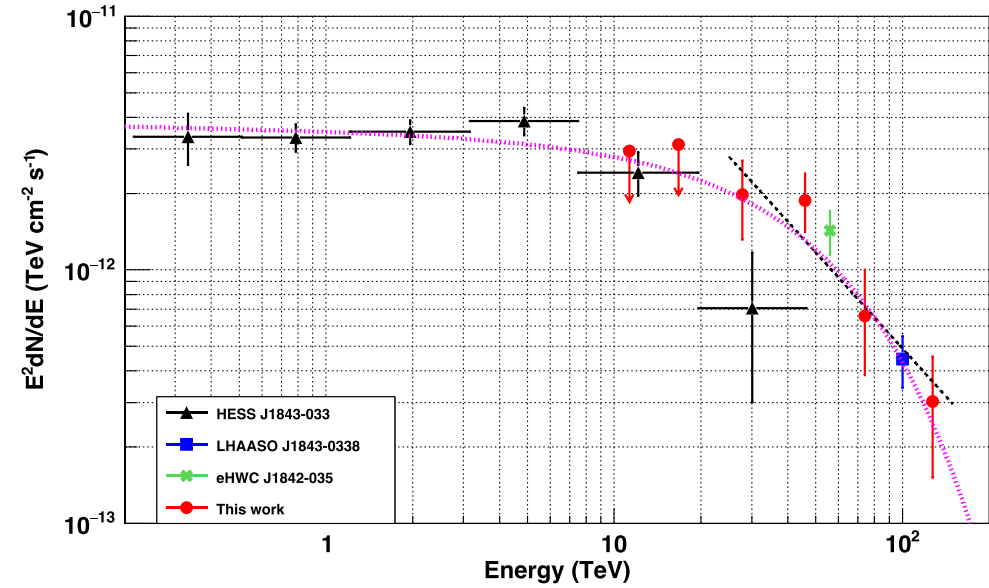
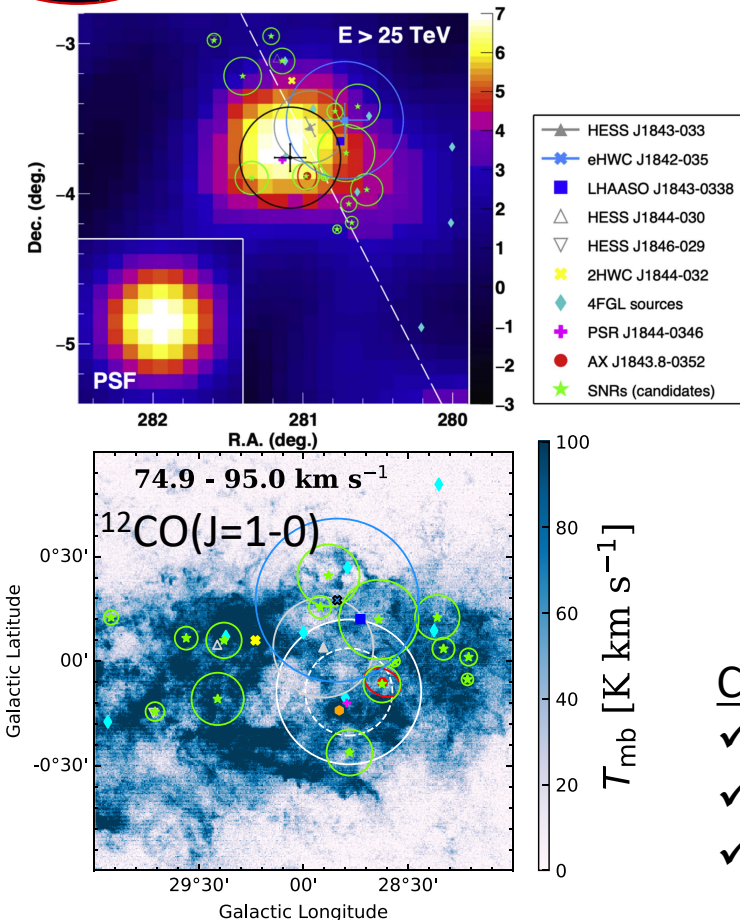
$$E_{\text{p,cut}} = \sim 500 \text{ TeV}$$

$$W_{\text{p}} = \sim 5 \times 10^{47} \text{ erg}$$



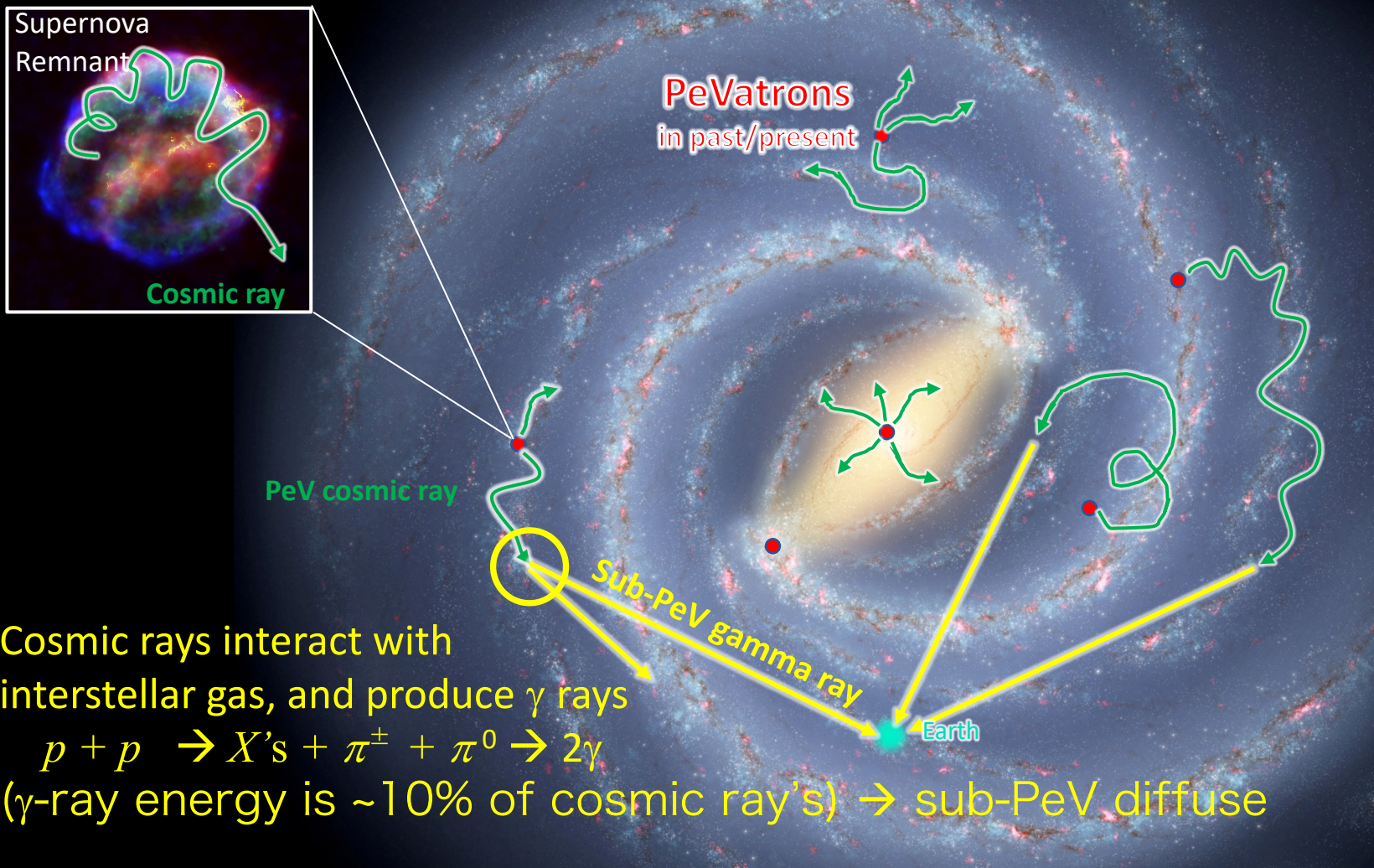
# PeVatron Candidate: HESS J1943-033

*Amenomori et al., ApJ, 932, 120 (2022)*



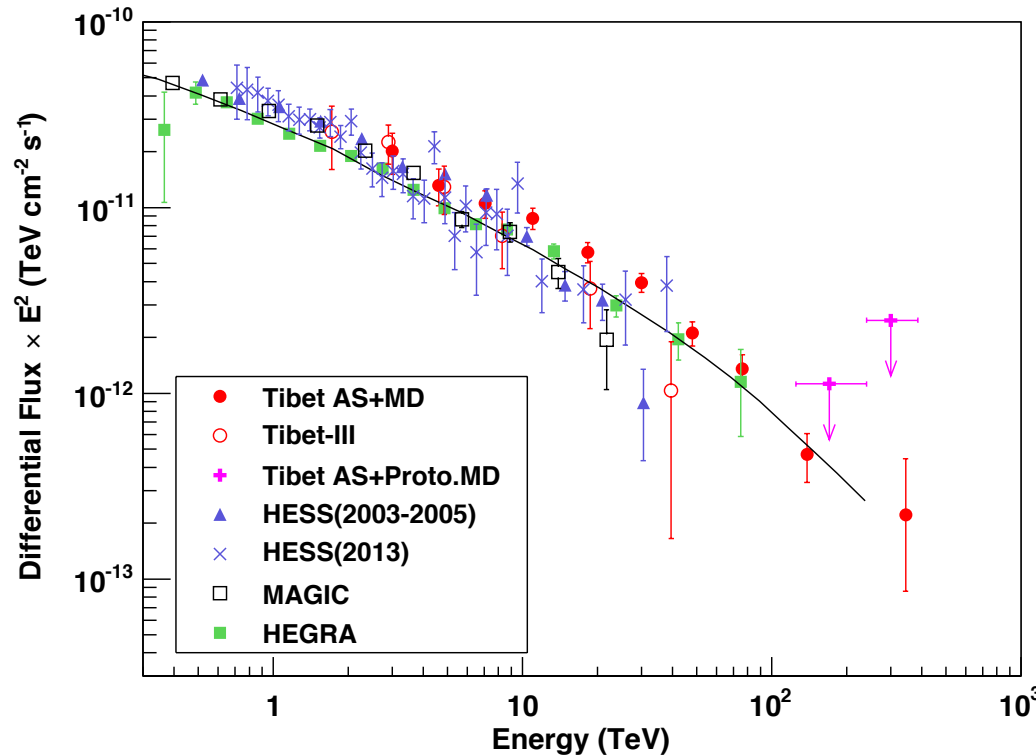
## Candidate sources

- ✓ Shell-type SNR G28.6+0.1?
- ✓ PSR J1844-00346?
- ✓  $\gamma$ -ray excess is coincident with the could and pulsar





# UHE $\gamma$ -rays from the Crab Nebula (2019)



*Amenomori+, PRL, 123, 051101, (2019)*

The highest energy  $\gamma \sim 450$  TeV

Thick curve :  
inverse Compton model  
normalized to HEGRA data

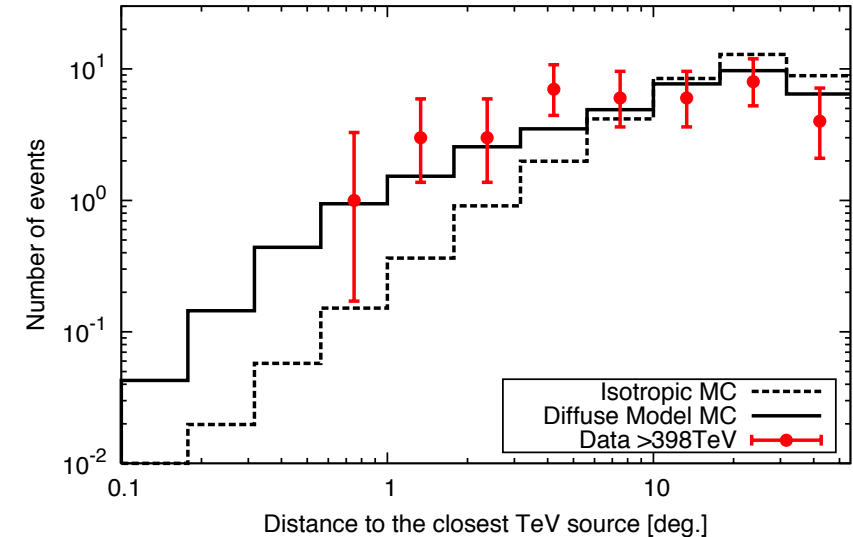
*Aharonian+, ApJ, 614, 897 (2004)*



# Correlation with known TeV Sources

Correlation between UHE  $\gamma$ -rays above 398 TeV and 60 galactic sources from TeVCat catalog including UNID, PWN , Shell, Binary, SNR..., excluding GRB, HBL, IBL, LBL, BL Lac, AGN, Blazar, FSRQ, FRI, Starburst)

- ✓ No excess around known TeV sources
- ✓ Event distribution is consistent with diffuse model



- ✓ High-energy  $e^{+/-}$  lose their energy quickly.
- ✓ Cosmic-ray protons can escape farther from the source.



Strong evidence for sub-PeV  $\gamma$  rays induced by cosmic rays

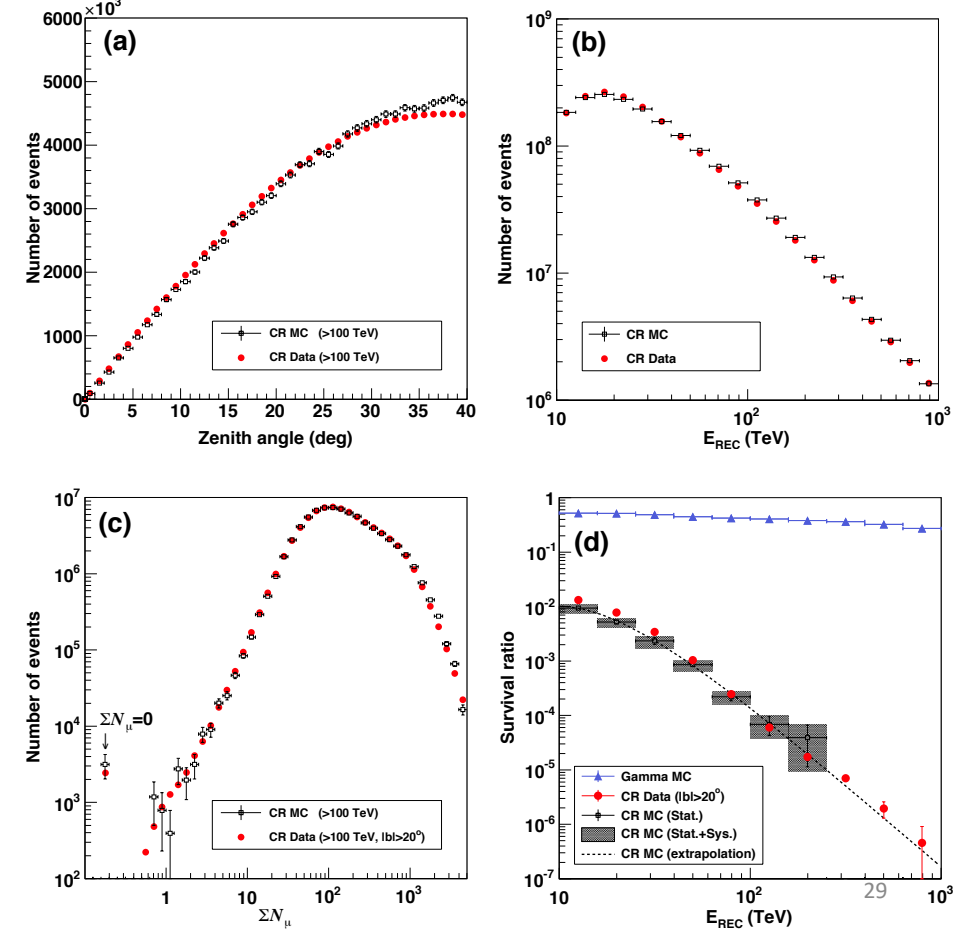


# Data/MC Comparison

- ✓ AS generation: CORSIKA
- ✓ Hadronic int. model:  
EPOS-LHC + FLUKA
- ✓ Detectors: GEANT4

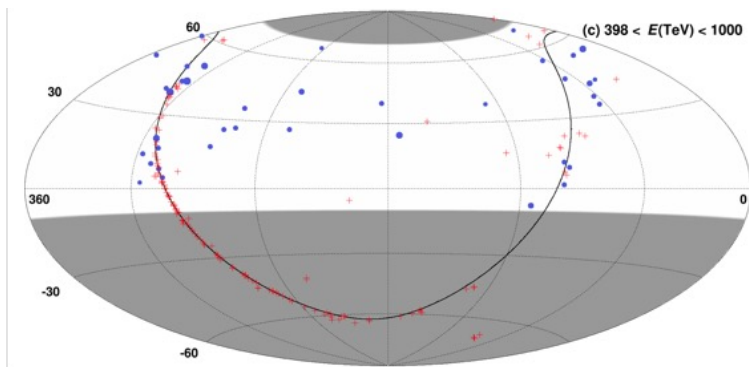
Reasonable agreement!

\*Note: Cosmic-ray MC simulation is not used for the flux calculation or for any optimization of the analysis.



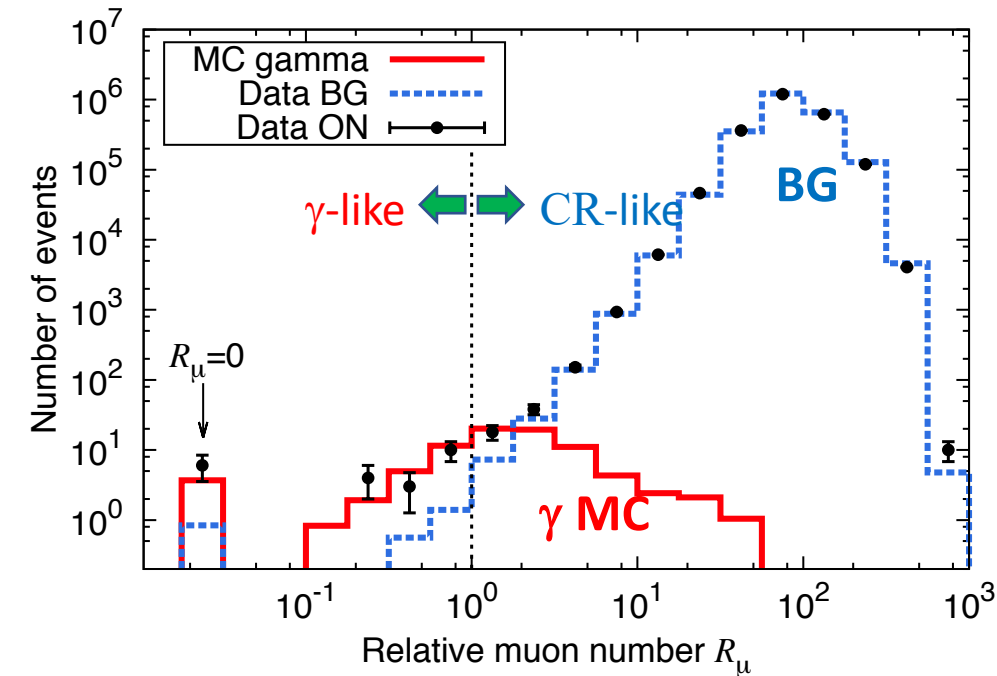


# Muon Number Distribution (>398 TeV)



- ON region  $|b| < 10^\circ$
- BG region  $|b| > 20^\circ$

Gamma Survival ratio :  
30% by MC sim (>398TeV)  
CR Survival ratio :  
 $\sim 10^{-6}$  ( $>398\text{TeV} = 10^{2.6}\text{TeV}$ )



$$R_\mu = \frac{\text{Observed } \# \text{ of muons}}{\# \text{ of muons at the cut value}}$$



# Data Table

TABLE S1. Number of events observed by the Tibet AS+MD array in the direction of the galactic plane. The galactic longitude of the arrival direction is integrated across our field of view (approximately  $22^\circ < l < 225^\circ$ ). The ratios ( $\alpha$ ) of exposures between the ON and OFF regions are 0.135 for  $|b| < 5^\circ$  and 0.27 for  $|b| < 10^\circ$ , respectively.

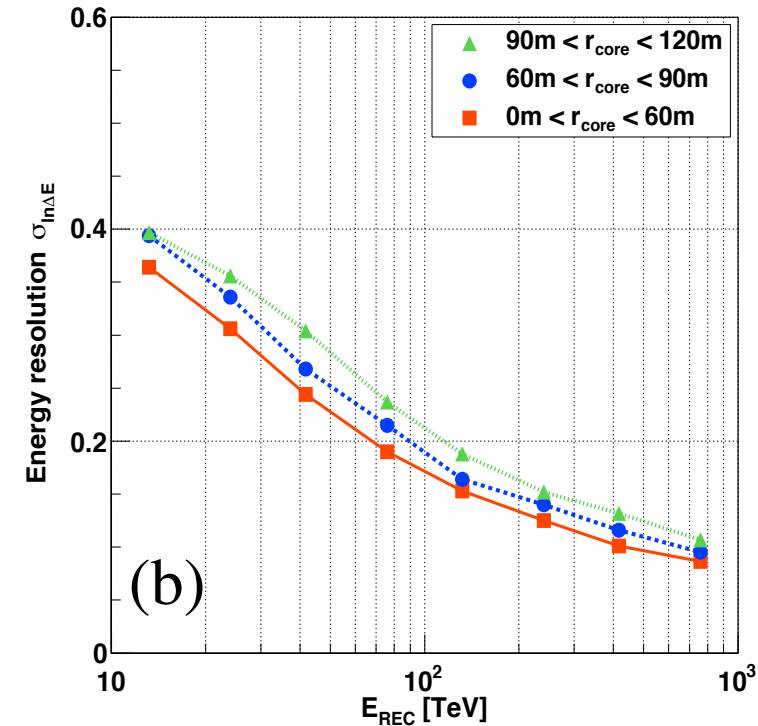
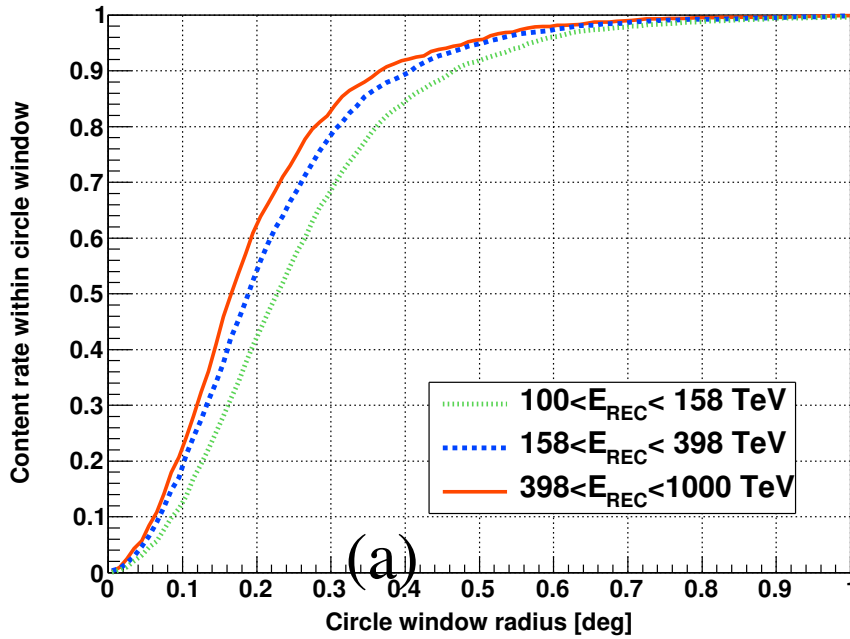
Energy bin (TeV)	$ b  < 5^\circ$			$ b  < 10^\circ$		
	$N_{\text{ON}}$	$N_{\text{BG}}$ (= $\alpha N_{\text{OFF}}$ )	Significance ( $\sigma$ )	$N_{\text{ON}}$	$N_{\text{BG}}$ (= $\alpha N_{\text{OFF}}$ )	Significance ( $\sigma$ )
100 – 158	513	333	8.5	858	655	6.6
158 – 398	117	58.1	6.3	182	114	5.1
398 – 1000	16	1.35	6.0	23	2.73	5.9

TABLE S2. Galactic diffuse gamma-ray fluxes measured by the Tibet AS+MD array.

Energy bin (TeV)	Representative $E$ (TeV)	Flux ( $25^\circ < l < 100^\circ,  b  < 5^\circ$ ) ( $\text{TeV}^{-1} \text{cm}^{-2} \text{s}^{-1} \text{sr}^{-1}$ )	Flux ( $50^\circ < l < 200^\circ,  b  < 5^\circ$ ) ( $\text{TeV}^{-1} \text{cm}^{-2} \text{s}^{-1} \text{sr}^{-1}$ )
100 – 158	121	$(3.16 \pm 0.64) \times 10^{-15}$	$(1.69 \pm 0.41) \times 10^{-15}$
158 – 398	220	$(3.88 \pm 1.00) \times 10^{-16}$	$(2.27 \pm 0.60) \times 10^{-16}$
398 – 1000	534	$(6.86^{+3.30}_{-2.40}) \times 10^{-17}$	$(2.99^{+1.40}_{-1.02}) \times 10^{-17}$



# Angular/Energy Resolutions



(b)



# CASA-MIA Observation

TABLE 1  
LIMITS TO DIFFUSE EMISSION

Region ( $50^\circ < l < 200^\circ$ )	Median Energy (TeV)	Significance ( $\sigma$ )	$J_\gamma/J_{\text{CR}}$	90% C.L. ( $10^{-5}$ )
$-2^\circ < b < 2^\circ$ .....	140	+1.78		7.2
	180	+1.81		3.8
	310	+2.56		5.2
	650	+1.12		3.2
	1300	+0.07		4.6
$-5^\circ < b < 5^\circ$ .....	140	+1.63		3.4
	180	+0.08		2.6
	310	+0.86		2.4
	650	+1.60		2.6
	1300	+0.06		3.5
$-10^\circ < b < 10^\circ$ .....	140	+2.39		2.8
	180	+1.79		2.2
	310	+0.87		2.3
	650	+0.91		1.8
	1300	-0.56		2.3

NOTE.—Tabulated upper limits to diffuse gamma-ray emission from the plane of the Galaxy. Although positive excesses are seen, we do not view these as statistically significant enough to claim detections. Flux limits are tabulated for bands along the Galactic plane from  $|b| < 2^\circ$  to  $|b| < 10^\circ$ . Median energy is quoted for integral flux limits. Selected spatial regions and energy bands are not statistically independent.

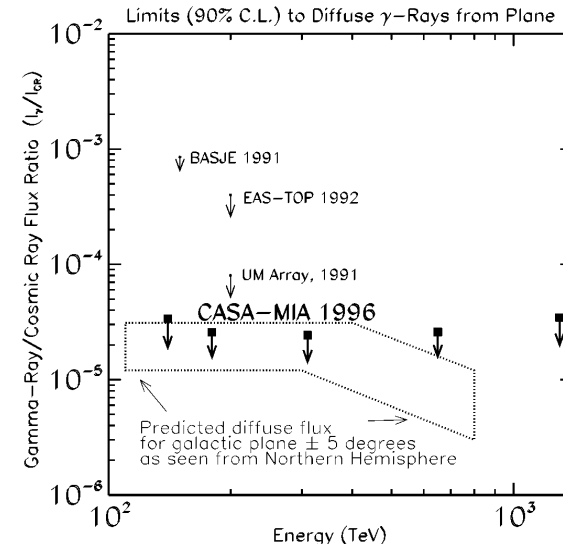


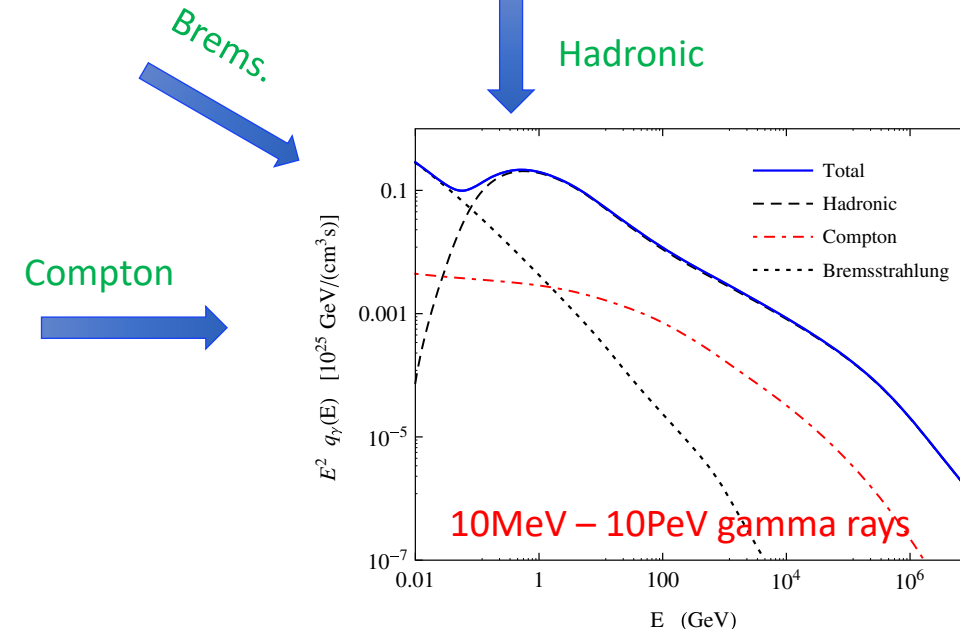
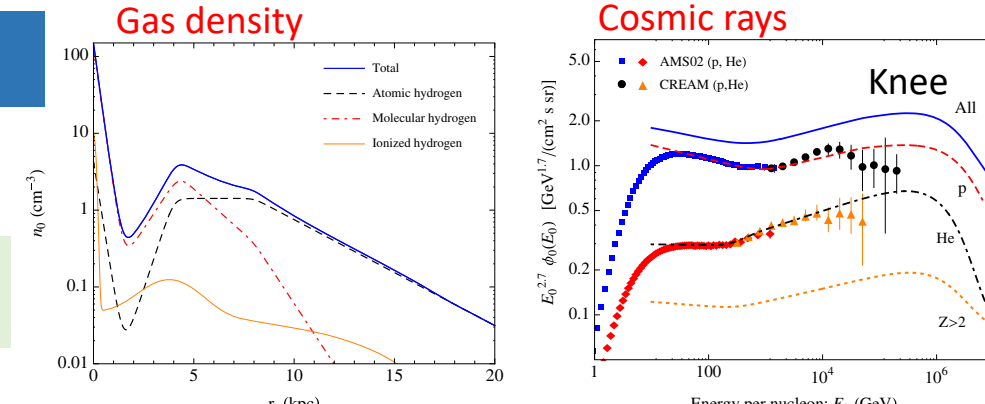
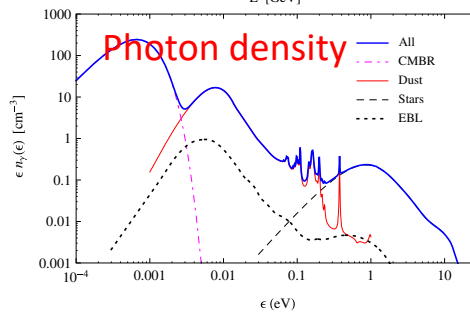
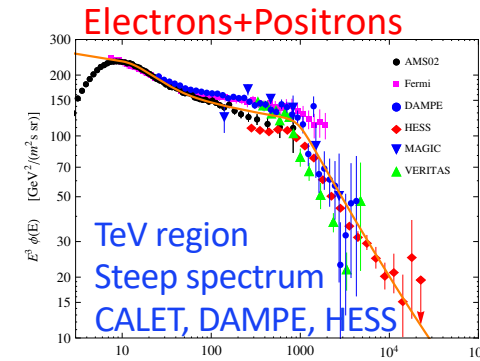
FIG. 4.—CASA-MIA sensitivity to diffuse gamma-ray emission from the central plane of the Galaxy ( $|b| < \pm 5^\circ$ ,  $50^\circ < l < 200^\circ$ ). Sensitivities are given in terms of the fraction of gamma rays relative to the detected all-particle flux of cosmic rays at the Earth. Also shown are limits from previous experiments (BASJE—Kakimoto et al. 1991; EAS-TOP—Aglietta et al. 1992, UM—Matthews et al. 1991). Predicted flux from Aharonian (1991).



# Diffuse Model

Lipari & Vernetto, PRD (2018)

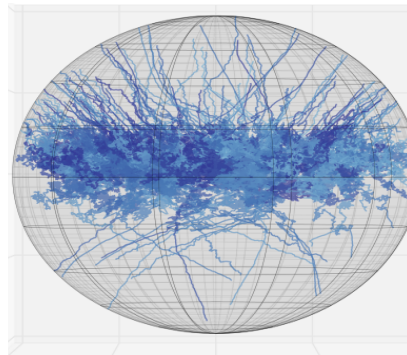
Model can reproduce global structure  
(not considered of the local structures)



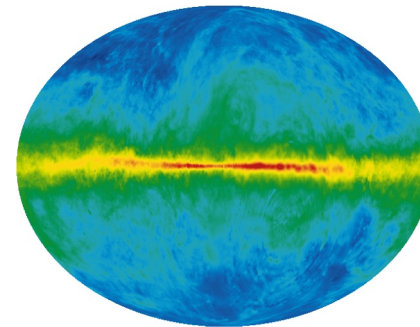


# Cosmic Ray Pool × ISM

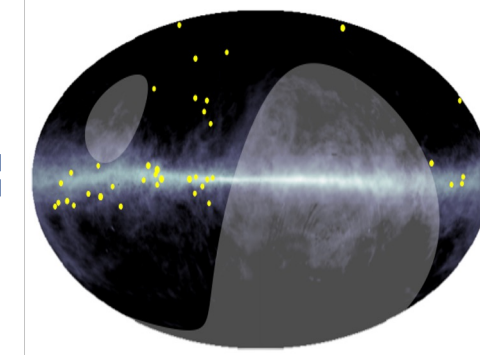
High-energy  
cosmic rays



Interstellar  
matter



High-energy  
gamma rays



**This Work**

Figure from slide presented by A. Kääpä (Bergische Universität Wuppertal) at CRA2019 workshop

Radio (21cm) HI Map  
Hartmann et al. (1997)  
Dickey & Lockman (1990)

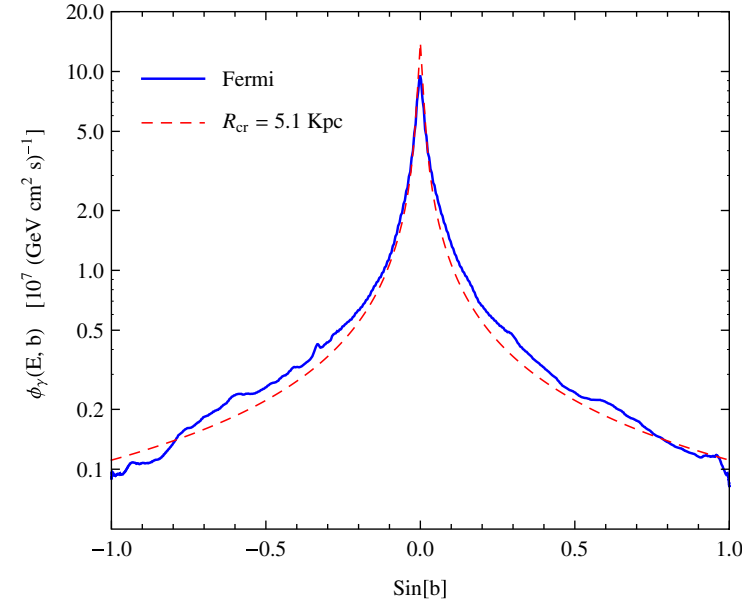
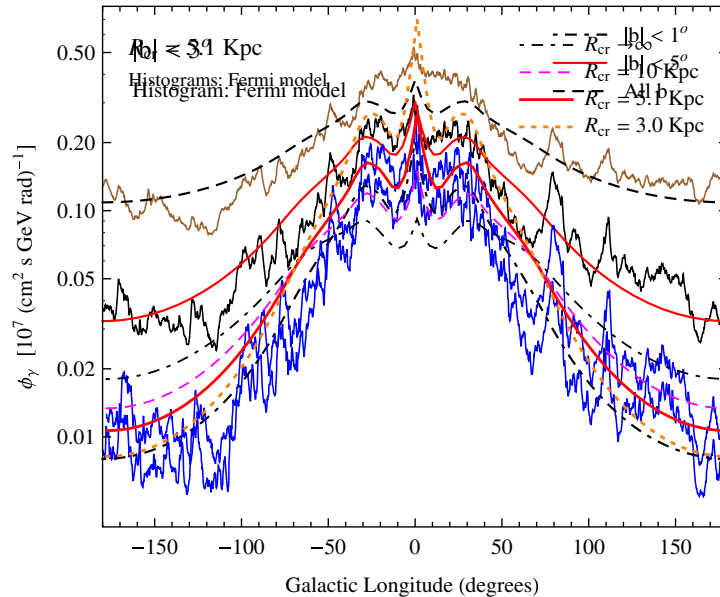
- ✓ This work proves a theoretical model that cosmic rays produced by PeVatrons are trapped in the Galactic magnetic field for millions of years, forming a pool of cosmic rays.



# Reproducing Fermi-LAT Results

Lipari & Vernetto, PRD (2018)

Model can reproduce global structure  
(not taken into account of local structure)

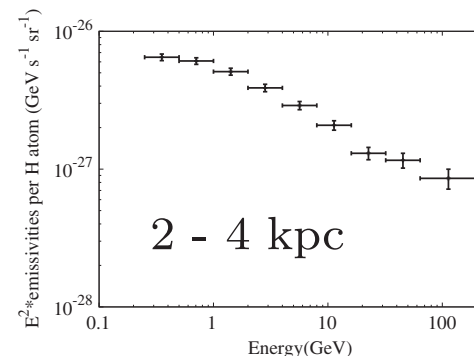
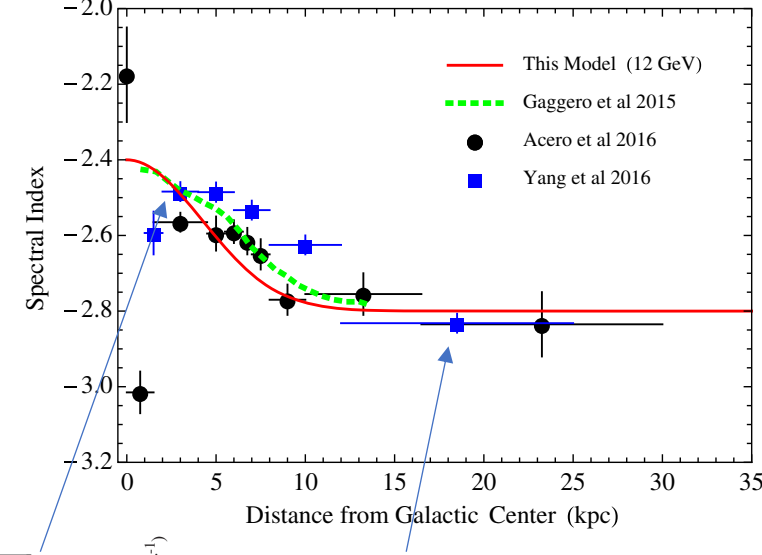




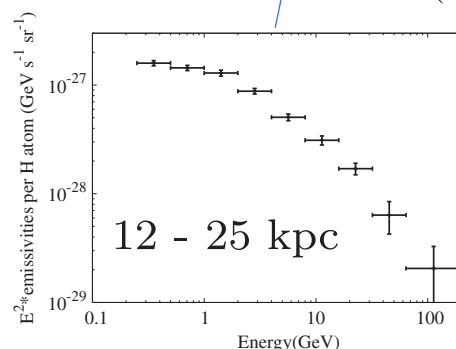
# Space Dependence of CR Spectrum

Lipari & Vernetto, PRD (2018)

Harder gamma-ray spectral index,  
getting closer to the G.C. @12 GeV

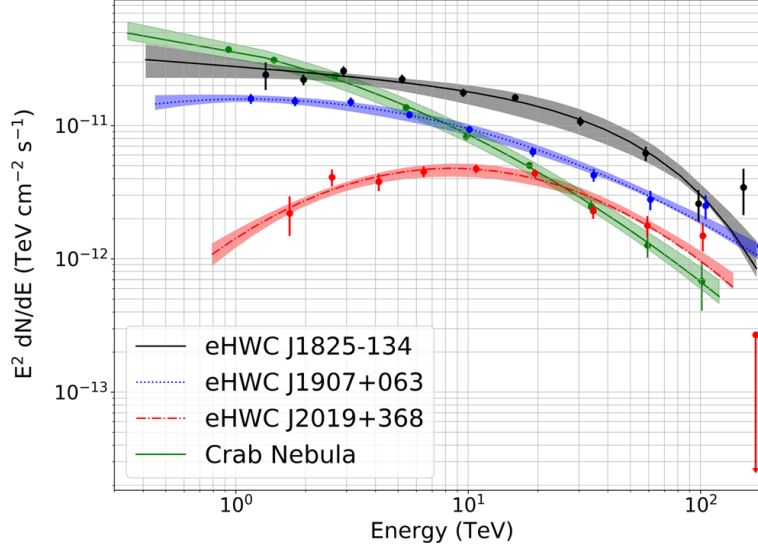


Yang et al., Phys. Rev. D 93, 123007 (2016)





# How to Identify PeVatrons



eHWC J1825-134 (PWN?)

PSR J1826-1334

PSR J1826-1256

A few SNRs ...

eHWC J1907+063 (PWN?)

PSR J1907+0602

SNR G40.5-0.5

eHWC J2019+368 (PWN?)

- ✓ Hard spectral index ( $\sim -2$ )
- ✓ Extended morphology

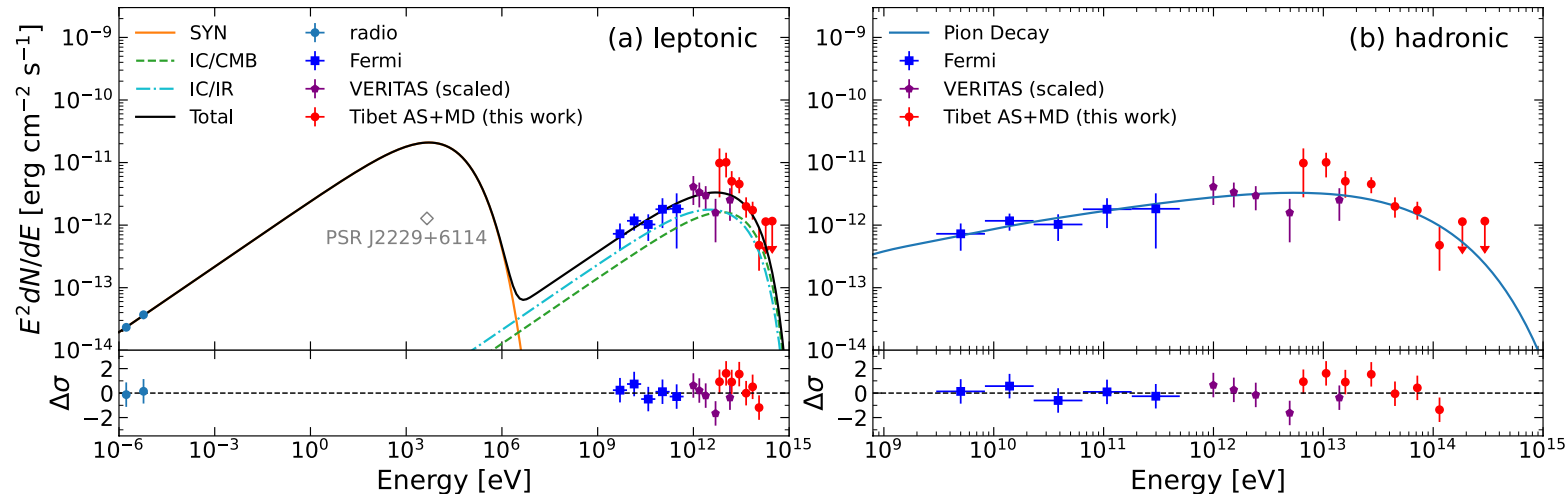


Source name	RA (°)	Dec (°)	Extension > 56 TeV (°)	$F$ (10 <sup>-14</sup> ph cm <sup>-2</sup> s <sup>-1</sup> )	$\sqrt{TS}$ > 56 TeV	Nearest 2HWC source	Distance to 2HWC source (°)	$\sqrt{TS}$ > 100 TeV
eHWC J0534 + 220	$83.61 \pm 0.02$	$22.00 \pm 0.03$	PS	$1.2 \pm 0.2$	12.0	J0534 + 220	0.02	4.44
eHWC J1809 – 193	$272.46 \pm 0.13$	$-19.34 \pm 0.14$	$0.34 \pm 0.13$	$2.4^{+0.6}_{-0.5}$	6.97	J1809 – 190	0.30	4.82
eHWC J1825 – 134	$276.40 \pm 0.06$	$-13.37 \pm 0.06$	$0.36 \pm 0.05$	$4.6 \pm 0.5$	14.5	J1825 – 134	0.07	7.33
eHWC J1839 – 057	$279.77 \pm 0.12$	$-5.71 \pm 0.10$	$0.34 \pm 0.08$	$1.5 \pm 0.3$	7.03	J1837 – 065	0.96	3.06
eHWC J1842 – 035	$280.72 \pm 0.15$	$-3.51 \pm 0.11$	$0.39 \pm 0.09$	$1.5 \pm 0.3$	6.63	J1844 – 032	0.44	2.70
eHWC J1850 + 001	$282.59 \pm 0.21$	$0.14 \pm 0.12$	$0.37 \pm 0.16$	$1.1^{+0.3}_{-0.2}$	5.31	J1849 + 001	0.20	3.04
eHWC J1907 + 063	$286.91 \pm 0.10$	$6.32 \pm 0.09$	$0.52 \pm 0.09$	$2.8 \pm 0.4$	10.4	J1908 + 063	0.16	7.30
eHWC J2019 + 368	$304.95 \pm 0.07$	$36.78 \pm 0.04$	$0.20 \pm 0.05$	$1.6^{+0.3}_{-0.2}$	10.2	J2019 + 367	0.02	4.85
eHWC J2030 + 412	$307.74 \pm 0.09$	$41.23 \pm 0.07$	$0.18 \pm 0.06$	$0.9 \pm 0.2$	6.43	J2031 + 415	0.34	3.07



# PeVatron Candidate: SNR G106.3+2.7

*Amenomori et al., Nat. Astron (2021)*



Electron spectrum:  $\alpha = -2.3$ ,  $E_{\text{cut}} = 190 \text{ TeV}$

Magnetic field:  $B = 8.6 \mu\text{G}$

→ Cooling time  $\tau_{\text{sync}} = 0.9 \text{ kyr} \ll \text{SNR age } 10 \text{ kyr}$

The required total energy of electrons is  $\sim 1.4 \times 10^{47} \text{ erg}$ , which only takes up  $\sim 2\%$  of the spin-down energy released in the entire pulsar lifetime. If the rest of the spin-down energy goes into the magnetic field, the average magnetic field in the PWN would be much larger than the required value of  $8 \mu\text{G}$  and results in very large fluxes at radio and X-ray wavelengths.



# Pulsar Halo Model of Diffuse $\gamma$ -Rays

Tim Linden and Benjamin J. Buckman, PHYSICAL REVIEW LETTERS 120, 121101 (2018)

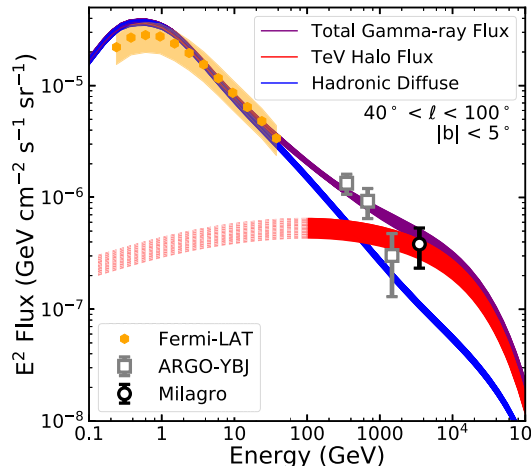


FIG. 1. The contribution of subthreshold TeV halos to the diffuse  $\gamma$ -ray emission along the galactic plane in the region  $40^\circ < \ell < 100^\circ$ , and  $|b| < 5^\circ$ , compared to observations by the Fermi-LAT (described in the text), ARGO-YBJ [5], and Milagro [1]. The background (blue) corresponds to the predictions of 128 GALPROP models of diffuse  $\gamma$ -ray emission [8]. The contribution from TeV halos (red) is described in the text. TeV halos naturally reproduce the TeV excess observed by Milagro, while remaining consistent with ARGO-YBJ observations. The dashed red region indicates our ignorance of low-energy  $\gamma$ -ray emission from TeV halos.

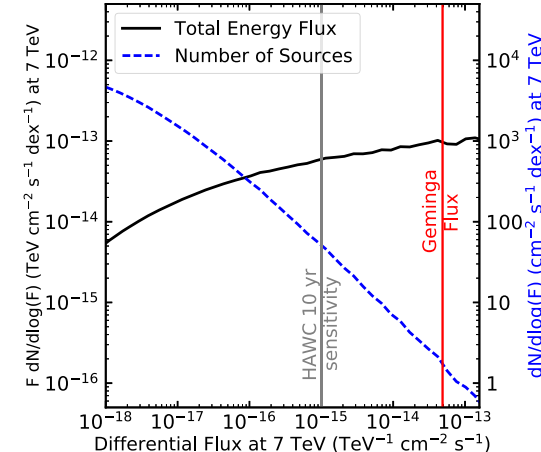
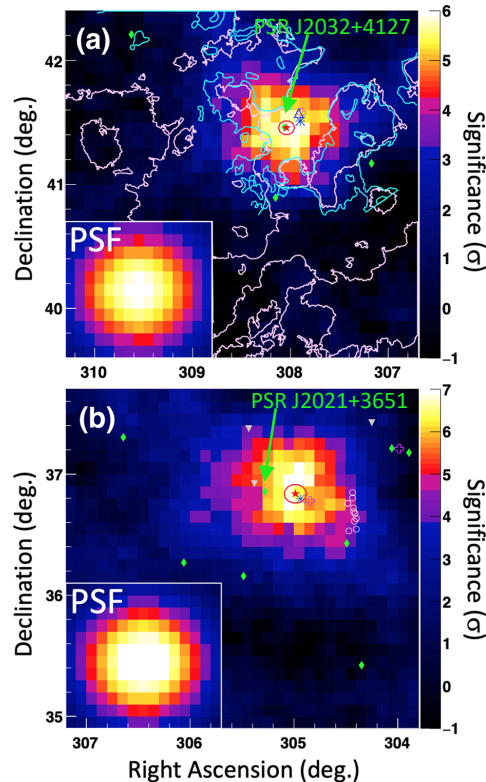


FIG. 3. The contribution of individual TeV halos to the TeV excess in the region  $40^\circ < \ell < 100^\circ$ , and  $|b| < 5^\circ$ . We normalize our results at 7 TeV [19], assuming that individual TeV halos convert their spin-down luminosity into 7 TeV  $\gamma$  rays with an identical efficiency as Geminga. Vertical lines correspond to the flux of Geminga, and the projected 10 yr HAWC sensitivity. Results are shown for the total  $\gamma$ -ray flux [ $F dN/d\log_{10}(F)$ , black, left y axis], which indicates that most of the  $\gamma$ -ray intensity stems from the bright TeV halos, as well as for the source count [ $dN/d\log_{10}(F)$ , blue, right y axis], which indicates that 10 yr HAWC data will observe  $\sim$ 50 TeV halos in the ROI. For illustrative purposes, in this plot we show the contribution from TeV halos with individual fluxes exceeding Geminga, predicting the existence of only  $\sim$ 1 such system.

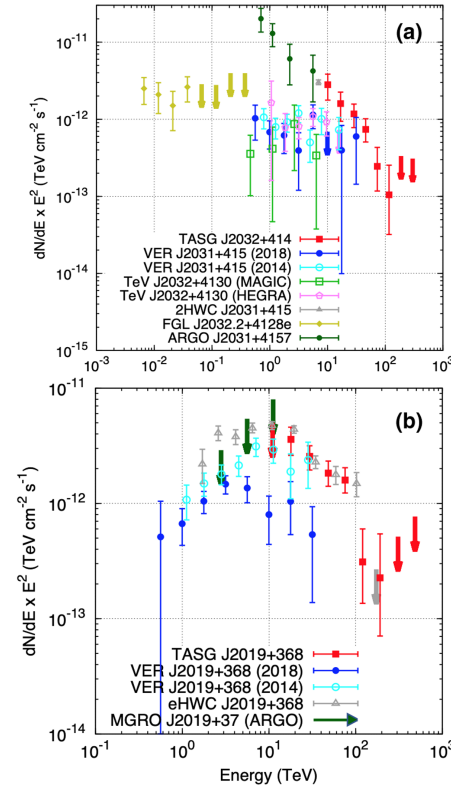


# Cygnus OB1 & OB2 in the 100 TeV region

Cyg. OB2



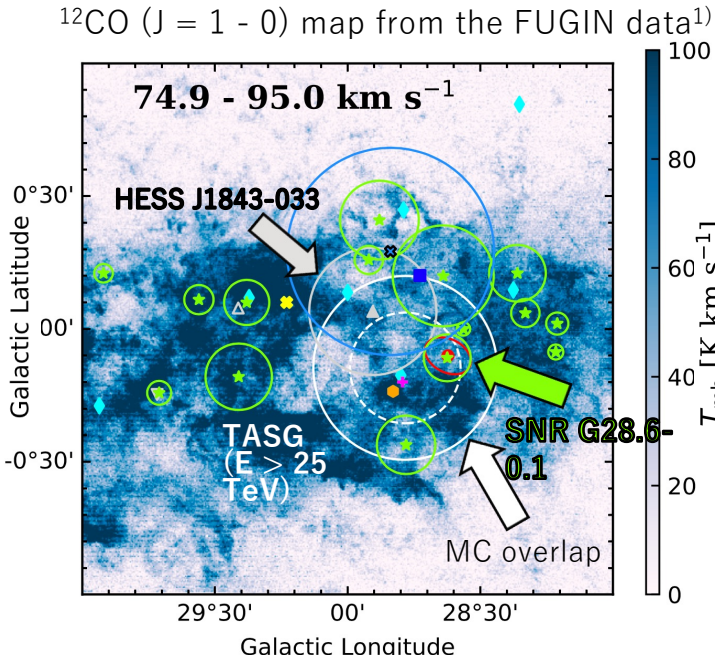
Cyg. OB1





# TASG J1844-038

## Discussion (1): Association of TASG J1844-038 w/ SNR G28.6-0.1 (2)



Several resemblances to SNR G106.3+2.7<sup>2)</sup>:

1. Overlapping molecular clouds (MCs),
2. Max. energy of CR protons:  $\approx 500\text{TeV}$ , &
3. Average of the estimated ages is  $\approx 10$  kyr.

=> Could have been a PeVatron in the past??

Diffusion time of CR protons through MCs<sup>3)</sup>:

$$\tau_{\text{diff}} = \frac{R_{\text{cl}}^2}{6D(E)} \sim 1.2 \cdot 10^4 \chi^{-1} \left( \frac{R_{\text{tot}}}{20\text{pc}} \right)^2 \left( \frac{E}{\text{GeV}} \right)^{-0.5} \left( \frac{B}{10\mu\text{G}} \right)^{0.5} \text{yr}$$

where R, size of MCs &  $\chi$ , suppression factor.

Assuming  $\chi = 0.1$  &  $B = 10\mu\text{G}$  ( $n_{\text{H}} \sim 100\text{ cm}^{-3}$ ),

$\tau_{\text{diff}}(R_{\text{TASG}}, E_{\text{CR}} > 250\text{ TeV}) \lesssim 2.0$  kyr &

$\tau_{\text{diff}}(R_{\text{HESS}}, E_{\text{CR}} \approx 10\text{ TeV}) \approx 4.9$  kyr.

Acceptable compared w/ the SNR's age

1) Umemoto et al., PASJ 69, 78 (2017)

2) Amenomori et al., Nat. Astron. 5, 460 (2021)

3) Gabici et al., Astrophys. Space Sci. 309, 365 (2007)



# Moon Shadow as a Calibration Source

- ✓ Tibet AS $\gamma$  experiment first time utilized the Moon shadow as the absolute energy calibration.

